Molecular characterization of Left-Right symmetry breaking in the mouse embryo

Richard C.V. Tyser[1,5], Ximena Ibarra-Soria[2,6], Monique Pedroza[1,7], Antonio M.A. Miranda[1,8], Teun A.H. van den Brand[3,9], Antonio Scialdone[3,10,11,12], John C. Marioni[2,3,4] and Shankar Srinivas[1, 13] *

[1] Department of Physiology, Anatomy and Genetics, University of Oxford, Oxford, OX1 3QX, UK.

[2] Cancer Research UK Cambridge Institute, University of Cambridge, Li Ka Shing Centre, Robinson Way, Cambridge, CB2 0RE, UK.

[3] European Molecular Biology Laboratory, European Bioinformatics Institute, Wellcome Genome Campus, Cambridge, CB10 1SD, UK.

[4] Wellcome Trust Sanger Institute, Wellcome Genome Campus, Cambridge, CB10 1SA, UK.

[5] Present address: Wellcome-MRC Cambridge Stem Cell Institute, University of Cambridge, Cambridge, UK.

[6] Present address: Genomic Sciences, GSK R&D, Stevenage, SG1 2NY, UK.

[7] Present address: Department of Genetics, Yale School of Medicine, Yale University, New Haven, CT 06510.

[8] Present address: National Heart & Lung Institute, Imperial Centre for Translational and Experimental Medicine, Imperial College London, London, W12 0NN, UK.

[9] Present address: Netherlands Cancer Institute, Plesmanlaan 12, 1066 CX Amsterdam.

[10] Present address: Institute of Epigenetics & Stem Cells, Helmholtz Zentrum München, D-81377 München, Germany.

[11] Present address: Institute of Functional Epigenetics, Helmholtz Zentrum München, D-85764 Neuherberg, Germany.

[12] Present address: Institute of Computational Biology, Helmholtz Zentrum München, D-85764 Neuherberg, Germany.

[13] Institute of Developmental and Regenerative Medicine, Department of Physiology, Anatomy and Genetics, Roosevelt Dr, Headington, Oxford OX3 7TY, UK

* author for correspondence: shankar.srinivas@dpag.ox.ac.uk

ABSTRACT

The asymmetric morphology of the mammalian heart is essential to its function as the organ of pulmonary and systemic double circulation. Left-right asymmetry is established by a leftward flow in the node that results in the asymmetric expression of *Nodal*. This triggers a cascade of asymmetric expression of downstream genes, such as *Pitx2c*, in the lateral plate mesoderm that gives rise to the first morphologically recognizable primordial heart structure, the cardiac crescent. Relatively little is known about gene expression asymmetries in the cardiac crescent that might underpin asymmetric cardiac morphogenesis. To systematically identify asymmetrically expressed genes, we performed a single-cell transcriptional analysis of manually dissected left and right halves of the cardiac crescent at stages spanning symmetry breaking. This revealed both left and right-sided genes that have not previously been implicated in left-right symmetry breaking. Some of these were expressed in multiple cell types but showed asymmetric expression in only a sub-set of cell types. We validated these findings using multiplexed *in situ* Hybridization Chain Reaction (HCR) and high-resolution volume imaging to characterize the expression patterns of select genes. Using *Dnah[iv/iv]* mutant embryos that show randomized situs, we established that all the genes tested tracked the asymmetric expression of *Pitx2c*, indicating their asymmetric expression also arose from the early asymmetries at the node. This study provides a high-fidelity molecular characterization of left-right symmetry breaking during cardiac crescent formation, providing a basis for future mechanistic studies on asymmetric cardiac morphogenesis.

INTRODUCTION

The vertebrate body plan is asymmetric, with most internal organs being asymmetrically shaped and positioned along the left-right (LR) body axis. These differences arise due to the regulation of several conserved genes early in development, around embryonic day (E) 7.5. Early bilateral symmetry breaking is initiated by the node[1]. The node is comprised of ciliated cells, which generate a leftward fluid flow that leads to the asymmetric activation of *Nodal*, a TGFβ growth factor, in the lateral plate mesoderm (LPM)[2–5]. Transient activation of *Nodal* results in the induction of transcription factors *Lefty* and *Pitx2*, which play a fundamental role in governing asymmetric organ morphogenesis[6–11]. Of the different *Pitx2* isoforms, it is the *Pitx2c* isoform that is asymmetrically expressed and, in contrast to transient *Nodal* expression, is maintained asymmetrically throughout organogenesis[12,13]. *Pitx2c* is the main cardiac isoform and is dynamically expressed during heart formation[14].

Heart formation is an excellent model to investigate LR differences as it is the first organ to form and function as well as display morphological asymmetries around E8.25[15]. In humans, defects in left-right asymmetry patterning lead to a range of congenital heart defects[16].

1

In the mouse, the heart initially forms as a symmetrical arc of cells, termed the cardiac crescent (CC), at around 7.75dpc before transitioning into the linear heart tube (LHT) which undergoes rightward looping prior to the formation of the four-chambered heart. The process of rightward looping and generation of a helical shape are modulated by *Nodal* at the poles of the LHT, which regulate proliferation, differentiation, and extracellular matrix genes[17]. Detailed morphological analysis and modeling of CC to LHT development has revealed that LR symmetry breaking can already be observed prior to rightward looping of the LHT, with LR differences detected in the orientation of the inflow tracts[18].

Whilst the morphological differences during heart looping have been well characterized, the early molecular basis is still relatively unclear[17,19,20]. We therefore sought to explore the temporal dynamics of LR molecular differences at the single-cell whole transcriptome level during cardiac crescent development and the onset of embryo wide symmetry breaking. To do this we exploited a single-cell transcriptomic dataset of the developing cardiac crescent that we had previously generated, in which we collected cells separately from the left and right cardiac regions. This dataset covers the period of development in which LR symmetry breaking is first established and allows the identification of novel asymmetrically expressed genes, thereby expanding our molecular understanding of how asymmetries arise in the forming embryo.

RESULTS

Identifying genes expressed asymmetrically in the forming cardiac crescent

Previously, we generated an unbiased single-cell transcriptomic dataset of the developing mouse heart, from emergence of the cardiac crescent to the formation of the linear heart tube, accessible at https://marionilab.cruk.cam.ac.uk/heartAtlas/ [21]. We identified twelve different cell populations, from all three germ layers. These included mesodermal cell types (cardiac progenitors, cardiomyocytes, endothelial and blood populations), overlying endoderm (including definitive and yolk sac) and adjacent ectoderm (representing surface/amnion and neuroectoderm)[21]. To discover left-right asymmetrically expressed genes, we manually dissected cells from the left or right sides of the embryos during the collection of cells from the cardiac crescent (Figure 1a). Thus, these data provide a highly time-resolved resource to investigate asymmetrically expressed genes during the onset of left-right asymmetry in the heart. Across the four stages of cardiac crescent development profiled, we generated high-quality transcriptomes for roughly equal numbers of cells from the left and right sides (Figure 1b). Most of the twelve cell subpopulations also had equal representation of cells from both sides, and these intermingled in the UMAP representation (Figure 1c, S1a). To confirm our dissection and faithful separation of the left and right cardiac crescent regions, we first examined the well-known asymmetrically expressed genes *Nodal*, *Lefty* and *Pitx2* (Figure 1d and S1b)[2,3,6–11]. These three genes were predominantly expressed in the cardiac mesoderm related clusters

(Me3-Me8), representing both cardiac progenitors and cardiomyocytes, and as expected, were expressed at significantly higher levels and in more cells from the left (Figure 1d and S1b). Cell cycle analysis showed no difference in the proportion of cells in G2/M, G1 or S-phase between left and right sides of the embryo in cardiomyocytes (Me3), blood (Me1), endothelial cells (Me2), endoderm (En1, En2) and 2) or ectoderm (Ec1, Ec2) although we observed a small but significant reduction of cells in G1 phase from the right side in the cardiac mesoderm progenitor clusters (Me4-7) (Figure 1e, S1c, Supplementary Table 1).

To identify novel asymmetrically expressed genes, we used differential expression analysis to test for expression differences between the left and right cells in each cell subpopulation (excluding Me1 and Me2 due to their small number of cells). In the mesodermal cell types, we identified 229 asymmetrically expressed genes, with two thirds expressed at higher levels in the cells from the left side of the embryo (Figure 1f and g, Supplementary Table 2). As observed before, *Lefty2* and *Pitx2* were among the most significant asymmetrically expressed genes, as well as *Atp1a1* and *Gal*, which has also been reported to be expressed at higher levels in the left side of the embryo[22]. The endodermal and ectodermal subpopulations showed fewer significant differences (23 and 60 respectively; Figure S2a and b, Supplementary Table 2). There was almost no overlap between the differentially expressed genes identified in each germ layer (only six genes were differentially expressed in the mesoderm clusters that were also differentially expressed in the endoderm (*Eif3b*, *Polr2a*, *Gm13050*) or in the ectoderm (*Gm18821*, *Efhd2*, *Klf6*), and none in all three.

The genes with asymmetric left-right expression in cardiac mesoderm cells (Me3-Me8) were expressed in varying patterns across the different clusters. Most DE genes were preferentially expressed either in the most mature cardiomyocytes (Me3; 58/229 genes) or in SHF progenitor cells (Me6-Me8; 72/229 genes; Supplementary Table 2). Interestingly, the genes with expression in the SHF-related clusters showed significantly larger fold-changes and smaller p-values compared to the genes in other clusters.

Validation of asymmetric expression using HCR

To experimentally validate the asymmetric expression of these genes, we used multiplexed Hybridization Chain Reaction (HCR) and confocal volume imaging. We used *Nkx2-5* and *Pitx2c* expression as positive controls for symmetrical and asymmetrical cardiac progenitor expression respectively. Multiplexed detection of these controls along with the transcript being tested allowed us to circumvent confounders that may have resulted from dynamic changes in expression patterns of these genes during development within even closely staged multiple samples.

To effectively use *Pitx2c* as a control for asymmetric expression, we first performed a detailed time-resolved characterization of its expression during early cardiac development stage mouse embryos. *Pitx2c* is the left specific isoform of *Pitx2* and has previously been reported to be expressed in the heart, gut and LPM[12,13]. To establish when and where asymmetric expression
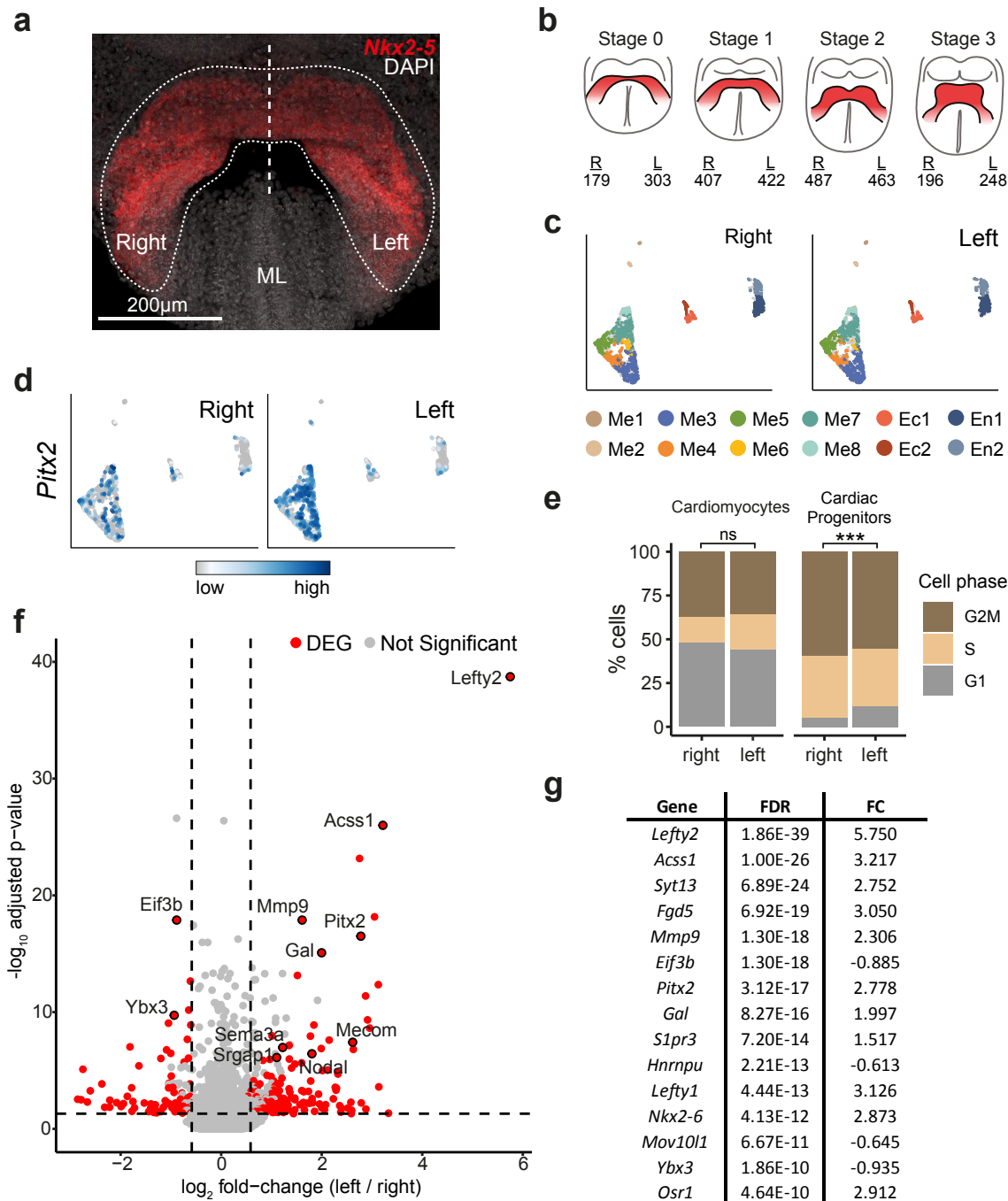
Figure 1: Single-cell molecular characterization of left right differences during cardiac crescent development. a, Ventral maximum intensity projection (MIP) of a stage 1 cardiac crescent stage embryo. The cardiac crescent is marked by NKX2-5 protein expression. The dotted region highlights the area micro-dissected for collecting cells and the L/R separation. ML, midline. **b**, Schematic of crescent stages collected for single-cell RNA-seq highlighting the number of cells collected from either the left or right that passed quality control. **c**, UMAP plot of all cells collected from either the left or right that passed quality control (n = 2,705) computed using highly variable genes. Cells with similar transcriptional profiles were clustered into 12 different groups, as indicated by the different colors, and were equally represented in both the left and the right. **d**, UMAP showing the expression of the well-characterized left-sided marker gene *Pitx2* in cells collected from either the left or right side of the forming cardiac crescent. **e**, Bar graphs showing the proportion of left and right cells from cardiomyocytes (Me3) and cardiac progenitors (Me4-Me7) in either G1, S or G2M phase of the cell cycle (binomial test that the proportion of cells in G1 is lower in the right side; ***p<0.001; ns = not significant). **f**, Differential expression analysis in mesodermal cell clusters (Me3-Me8). The adjusted p-value (y-axis) is plotted against the fold-change between left-right cells (x-axis). For non-differentially expressed genes (grey), the average fold-change for all clusters is used; for DEGs (red) the largest fold-change (in clusters where the gene is expressed) is used. Genes are considered DE if their adjusted p-value is lower than 0.05 and their fold-change is larger than 1.5 (indicated by the dashed lines) in at least one cluster. **g**, Table showing the top 15 DEGs, along with false discovery rate (FDR) and largest (absolute) log2 fold change (FC) when comparing left to right sided cells.

of *Pitx2c* first occurs during cardiac crescent formation, we used whole mount multiplexed in situ HCR, followed by confocal volume imaging (Figure 2a). This showed that in the majority of late headfold stage embryos[23] (stage -1 cardiac crescents) *Pitx2c* was LR symmetrically expressed (Figure 2a) in all tissues (10/12 embryos). *Pitx2c* transcripts were detected in the cranial mesoderm, yolk sac endoderm, paraxial mesoderm and headfold ectoderm (Figure 1d, 2a and S3a-c). In a minority of embryos (2/12), *Pitx2c* was detected asymmetrically in a small region of left caudal LPM, closest to the node and furthest from
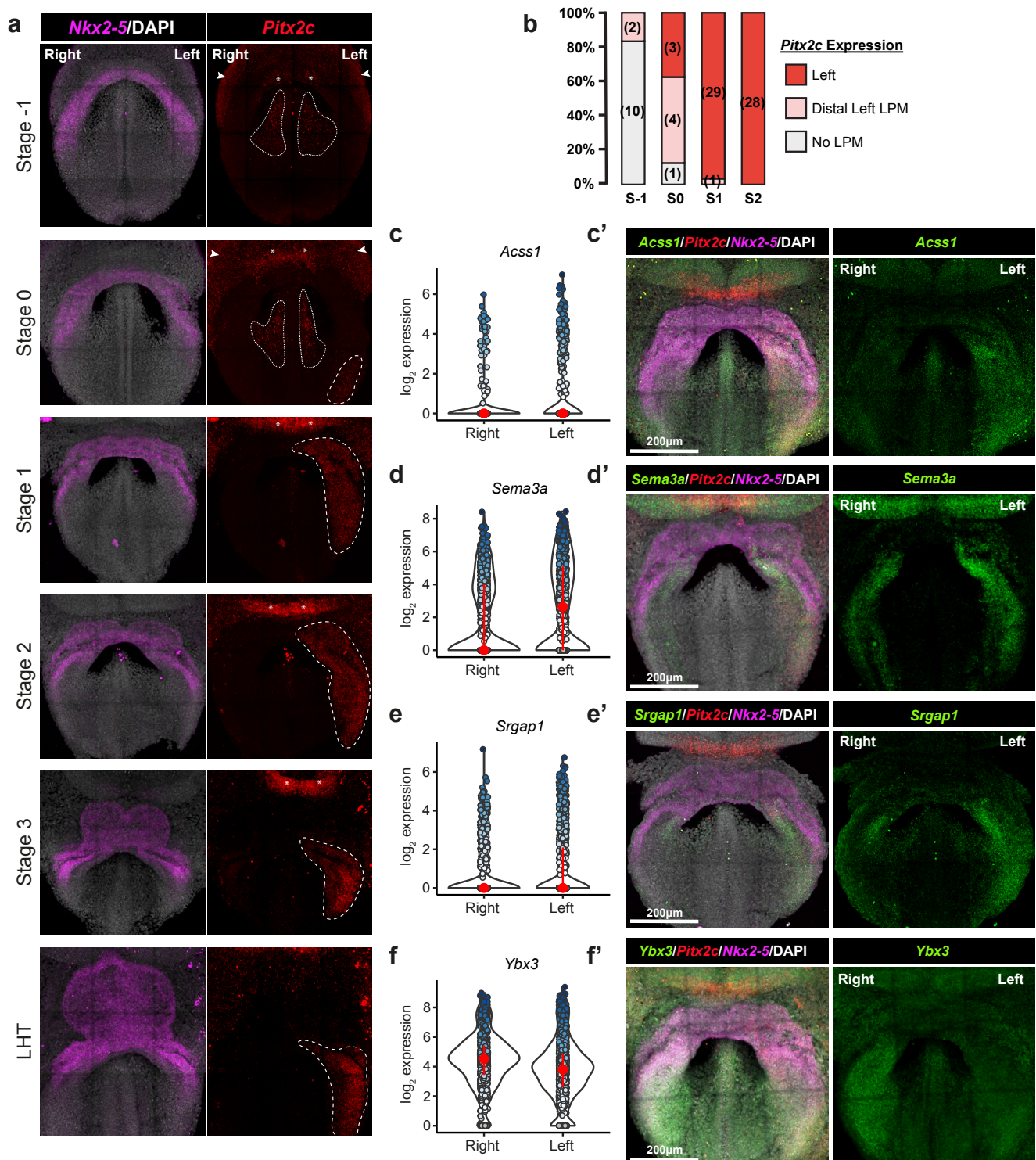
Figure 2: Identification and validation of asymmetrically expressed genes. a, MIPs covering stages of cardiac crescent development showing expression of *Nkx2-5* and *Pitx2c* using Hybridization Chain Reaction. *Pitx2c* expression is detected in the lateral plate mesoderm (dashed regions), paraxial mesoderm (dotted regions), yolk sac endoderm (arrowheads) and ectoderm (asterisks) at varying stages of crescent development. **b**, Quantification of asymmetry in *Pitx2c* expression at different stages of cardiac crescent development. A total of 78 embryos were quantified across stages -1 to 2 of crescent development; numbers per stage shown in brackets. **c-f**, Violin plots showing the expression of *Acss1*, *Sema3a*, *Srgap1*, and *Ybx3* in left and right mesodermal cells. Darker blue dots represent single cells with higher expression. **c'-f'**, Maximum Intensity Projection (MIP) of hybridization chain reaction (HCR) staining revealing the expression pattern of selected genes as well as *Pitx2c* and *Nkx2-5* as controls, thus validating computational observations. Individual channels are shown in Supplementary Figure 5.

the cardiac crescent. At stage 0, *Pitx2c* expression remained symmetrical in the paraxial and cranial mesoderm, headfold ectoderm and yolk sac endoderm (Figure 2a). However, by this stage, *Pitx2c* was detected asymmetrically in left-sided LPM in a majority of embryos (7/8), either in a small left-sided region of caudal LPM (4/7 embryos) or had begun to spread rostrally throughout the left-sided LPM extending into

the maturing cardiac crescent (3/7 embryos) (Figure 2a and S3d-i). By stage 1, most embryos (29/30) showed left-asymmetric expression throughout the LPM. Symmetric *Pitx2c* expression was still maintained in the headfold ectoderm, cranial mesoderm and yolk sac endoderm, but was lost from the paraxial mesoderm below the crescent (Figure 2a and S4). Once the linear heart tube had formed, asymmetric *Pitx2c* expression

was restricted to the left sinus horn and LPM, whilst symmetric expression was maintained in the headfolds, cranial mesoderm and yolk sac. This reveals that the expression of *Pitx2c* is extremely dynamic over the approximately 10-hour period spanning stages -1 to LHT (Figure 2b).

Next, we selected five left-sided genes identified from the single-cell RNA-seq dataset to test: *Acss1*, *Mmp9*, *Mecom*, *Sema3a* and *Srgap1*. HCR analysis was initially performed on mid cardiac crescent stage (stages 1–3) embryos, when *Pitx2c* was clearly asymmetrically expressed. All the left-sided genes tested showed left-sided asymmetry, but their expression profiles differed. *Acss1*, which encodes a mitochondrial acetyl-CoA synthetase enzyme, was predominantly expressed in the left LPM (10/10 stage 1–3 embryos), extending into the cardiac crescent, with diffuse expression throughout this region (Figure 2c, S5 and S6a). In contrast, *Sema3a*, encoding a member of the semaphorin signaling family, and *Srgap1*, encoding the SLIT-ROBO Rho GTPase Activating Protein 1, were expressed in both the left and right LPM extending into the cardiac crescent, but in all cases, more strongly on the left (*Sema3a*; 6/6 stage 1–3 embryos, *Srgap1*; 7/8 stage 1–3 embryos) (Figure 2d, 2e, S5 and S6a). *Sema3a* also showed strong symmetrical expression within the headfolds, consistent with its expression in the transcriptional clusters Ec1 and 2 (Figure S6a).

Mecom, which encodes the transcription factor EVI1, was identified in two mesodermal clusters, Me2 (endocardium) and Me6 (differentiating cardiac progenitors). *Mecom* was symmetrically expressed in cluster Me2 and asymmetrically expressed in cluster Me6 (Figure 3a). HCR validated this and showed strong left-asymmetric expression in the LPM (9/9 stage 1–3 embryos) but symmetrical expression in the forming endocardial cells within the cardiac crescent (Figure 3b, 3c and S6a). *Mmp9*, which encodes a matrix metalloprotease involved in extracellular matrix remodeling, was detected within individual cells in the left limb of the cardiac crescent (12/12 stage 1–3 embryos) (Figure 3d, 3e and S6). At slightly later LHT stages, *Mmp9* continues to be asymmetrically expressed and is downregulated in *Nodal* mutants[17]. The anatomical characterization and validation of left-sided expression of *Acss1*, *Mmp9*, *Mecom*, *Sema3a*, *Srgap1* confirms our single-cell transcriptional approach to identify novel asymmetrically expressed genes.

Our computational analysis also revealed right-sided genes (Figure 1f and 1g), though fewer than left-asymmetric genes. We sought to experimentally validate *Ybx3* and *Eif3b* by HCR. *Ybx3* encodes a DNA- and RNA-binding protein which can regulate transcription and mRNA stability, having a role in proliferation and amino acid uptake[24]. *Ybx3* was expressed in all germ layers including all mesoderm cell types, however it showed significantly greater expression in mesodermal cells collected from the right side (Figure 2f, S5 and S6a). Whole mount HCR imaging revealed the widespread expression of *Ybx3* in tissues derived from all germ layers. Furthermore in 6/9 embryos, it was expressed more strongly in the right LPM compared to the left, whilst the remaining embryos showed symmetrical (2/9) or left-sided expression

(1/9) (Figure 2f). We also assessed the right-sided expression of *Eif3b* that encodes the RNA-binding component of the eukaryotic translation initiation factor 3 complex required for protein synthesis initiation. *Eif3b* was strongly expressed in all cell clusters, and this was supported by HCR analysis which revealed strong expression throughout all tissues (Figure S4). Right-sided *Eif3b* expression was detected in 3 out of 6 embryos, with the remaining embryos displaying left-right symmetrical expression.

Timing of origin of asymmetries in gene expression

To address the timing with which asymmetrical expression of these genes manifested during the emergence of left-right asymmetry, we performed HCR at earlier stages. We also measured *Pitx2c* expression, to determine whether asymmetric expression of these novel genes preceded or followed that of *Pitx2c*. This revealed that all the markers tested showed asymmetric expression only after *Pitx2c* was upregulated in caudal left-side of the embryo (Figure 4). *Acss1* was not expressed at all prior to asymmetric *Pitx2c* expression. *Mmp9* expression was detected in individual cells located symmetrically on both the left and right sides of the embryo at stages when *Pitx2c* was starting to be expressed asymmetrically in the left LPM. As previously reported, *Mecom* had two different domains of expression. As asymmetric *Pitx2c* expression became established, endothelial *Mecom* expression was detected symmetrically but there was no expression in the LPM. At a stage when *Pitx2c* was starting to be expressed asymmetrically in the left LPM, *Srgap1* was expressed symmetrically in the LPM, more rostrally than the asymmetric LPM *Pitx2c* expression. At this stage, *Sema3a* was strongly expressed in both the left and right sides of the neural ectoderm as well as the LPM running caudally from the cardiac crescent (Figure 4). Whilst there was some overlap in the expression of *Sema3a* and *Nkx2-5* at the boundary of the cardiac crescent, *Sema3a* was expressed only at low levels in the cardiac crescent as well as in the cranial and paraxial mesoderm (Figure 4 and S7).

Left-right asymmetric gene expression is triggered by events at the node dependent on leftward flow created by the action of nodal cilia[1,25]. Inversus viscerum (iv) mutant embryos have defective nodal cilia and randomized situs due to a mutation in *Dnah11*, the gene encoding the dynein axonemal heavy chain 11[26–28]. To test the dependence of the asymmetric expression of *Mecom* on nodal ciliary action, we looked at *Mecom* expression in *Dnah11*[iv/iv] embryos. Since *Mecom* shows both symmetric (endocardium) and asymmetric (myocardial progenitors in LPM) expression within the forming heart, it offers a particularly interesting candidate to specifically study the asymmetric cardiac expression, using the symmetric component of expression as an internal control.

Homozygous *Dnah11*[iv/iv] mutants are viable and have been described based on gross morphology to show a range of phenotypes ranging from *situs solitus* to *situs inversus totalis*[26,27]. We first performed a detailed molecular characterization of the left-right phenotype of these mutants during cardiac development stages, using *Pitx2c* expression as a
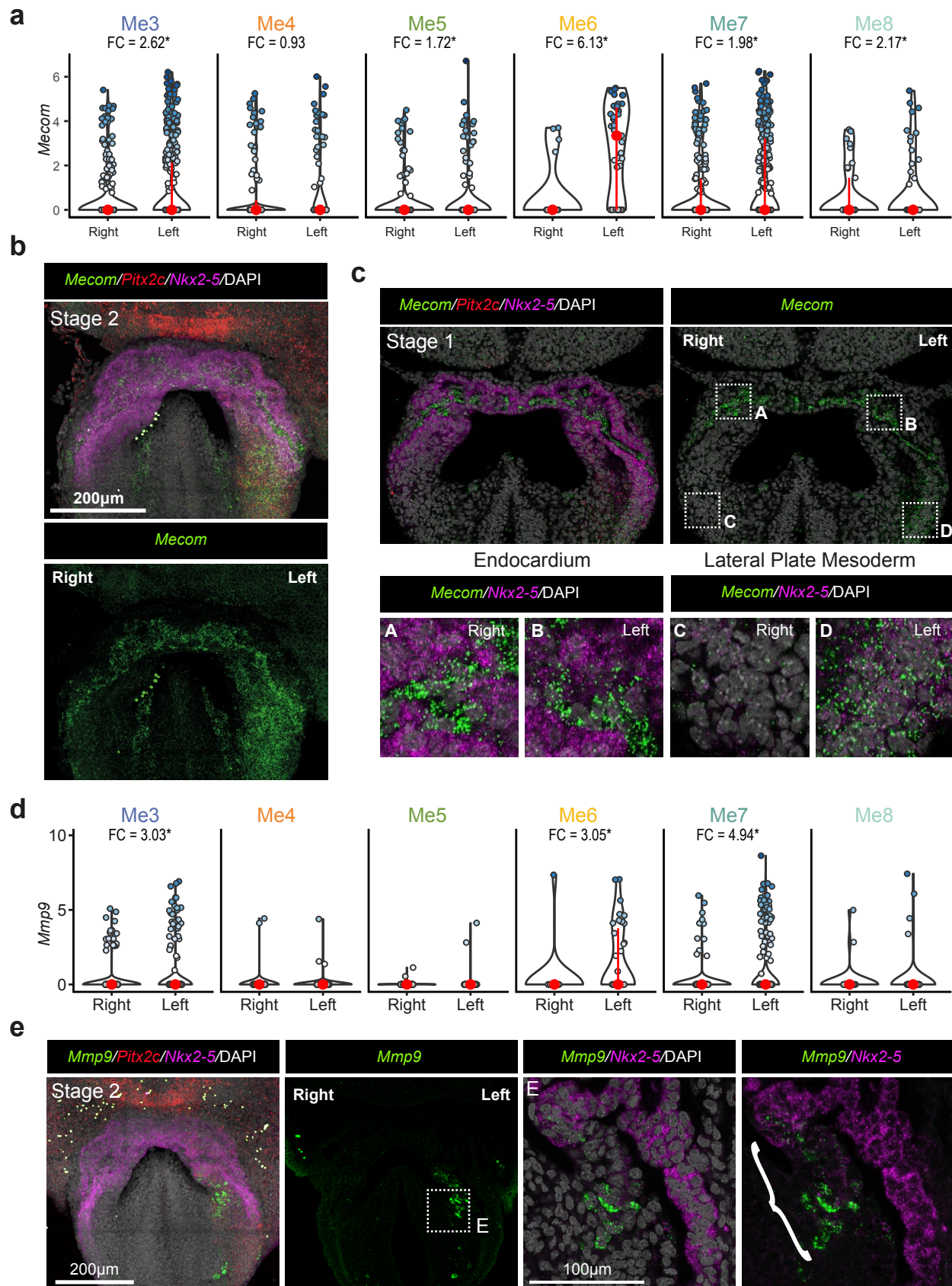
Figure 3: Asymmetrical gene expression varies depending on mesodermal cell type. a, Violin plots showing the expression of *Mecom* in the different mesodermal clusters. Darker blue dots represent single cells with higher expression. Changes were considered significant if the fold change (in brackets) was above 1.5 but only for clusters in which the gene was detected at moderate levels. **b**, Maximum Intensity Projection (MIP) of a hybridization chain reaction (HCR) staining revealing the expression pattern of *Mecom*, *Pitx2c* and *Nkx2-5* in a stage 2 cardiac crescent embryo. **c**, Single Z section of a HCR staining for *Mecom*, *Pitx2c* and *Nkx2-5* highlighting the symmetrical expression of *Mecom* in the forming endocardium (Me2; insets A and B) and asymmetrical expression in the lateral plate mesoderm (Me3, Me5-8; insets C and D). **d**, Same as a, but for *Mmp9*. **e**, MIP of a HCR staining revealing the expression pattern of *Mmp9*, *Pitx2c* and *Nkx2-5* in a stage 2 cardiac crescent embryo. Single Z section (inset E) showing the expression of *Mmp9* in single cells corresponding to progenitor clusters Me6 and Me7 (bracket).
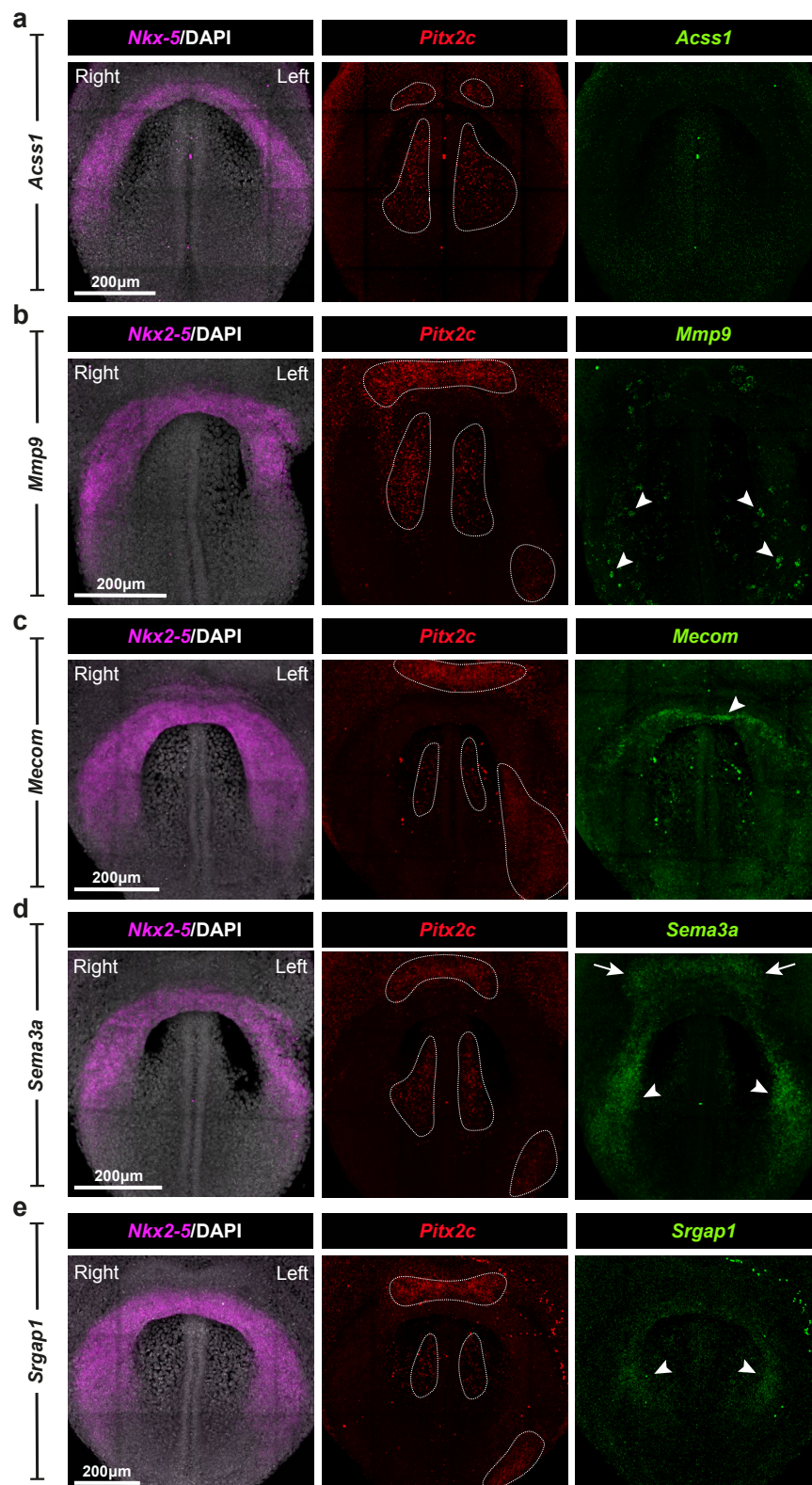
Figure 4: Expression of newly identified asymmetrically expressed genes during the onset of symmetry breaking. **a-e**, Maximum Intensity Projections (MIP) of hybridization chain reaction (HCR) staining revealing the expression pattern of *Acss1* (**a**), *Mmp9* (**b**), *Mecom* (**c**), *Sema3a* (**d**) and *Srgap1* (**e**), as well as *Pitx2c* and Nkx2-5, in embryos at the initiation of asymmetry breaking. Dotted regions highlight the symmetrical expression of *Pitx2c* in the ectoderm and paraxial mesoderm as well as expression in the left caudal lateral plate mesoderm (LPM). Arrowheads mark: individual *Mmp9* expressing cells (**b**); symmetrical Mecom expression in the endocardium (**c**); symmetrical *Sema3a* and *Srgap1* expression in LPM (**d** and **e**). Arrows mark *Sema3a* expression in the ectoderm (**d**).

readout of situs. In homozygous mutant embryos between stage 0 and LHT (n=90), *Pitx2c* showed four different expression profiles as previously reported[29]: left-asymmetric expression (32.22%), right-asymmetric expression (31.11%), symmetric expression (14.44%) and no expression (22.22%) (Figure 5a and 5c). During cardiac crescent to LHT maturation there was a shift in the proportion of embryos displaying a given *Pitx2c* expression profile (Figure 5b). In mutant embryos, the onset of asymmetric *Pitx2c* expression was delayed in comparison to that of wild type embryos, with asymmetric expression being detected only from stage 1 onwards. As the cardiac crescent transitioned into the LHT, the proportion of embryos with symmetrical *Pitx2c* expression increased, whilst the number of embryos

with no *Pitx2c* expression decreased.

When we looked at *Mecom* expression in these embryos, we observed normal symmetrical expression in the cardiac endothelium in all *iv/iv* mutant embryos irrespective of the expression pattern of *Pitx2c*. In mutant embryos in which *Pitx2c* was expressed asymmetrically in either the right or left LPM, we found that the LPM expression of *Mecom* correlated with the pattern of expression of *Pitx2c* (Figure 5c). In embryos where no *Pitx2c* expression was detected in the LPM, *Mecom* could only be detected in endothelial cells and was not expressed in LPM, whilst in embryos with symmetrical *Pitx2c* expression in the LPM, *Mecom* too was expressed symmetrically in the left and right LPM. Overall, these results indicate that *Mecom* expression

7
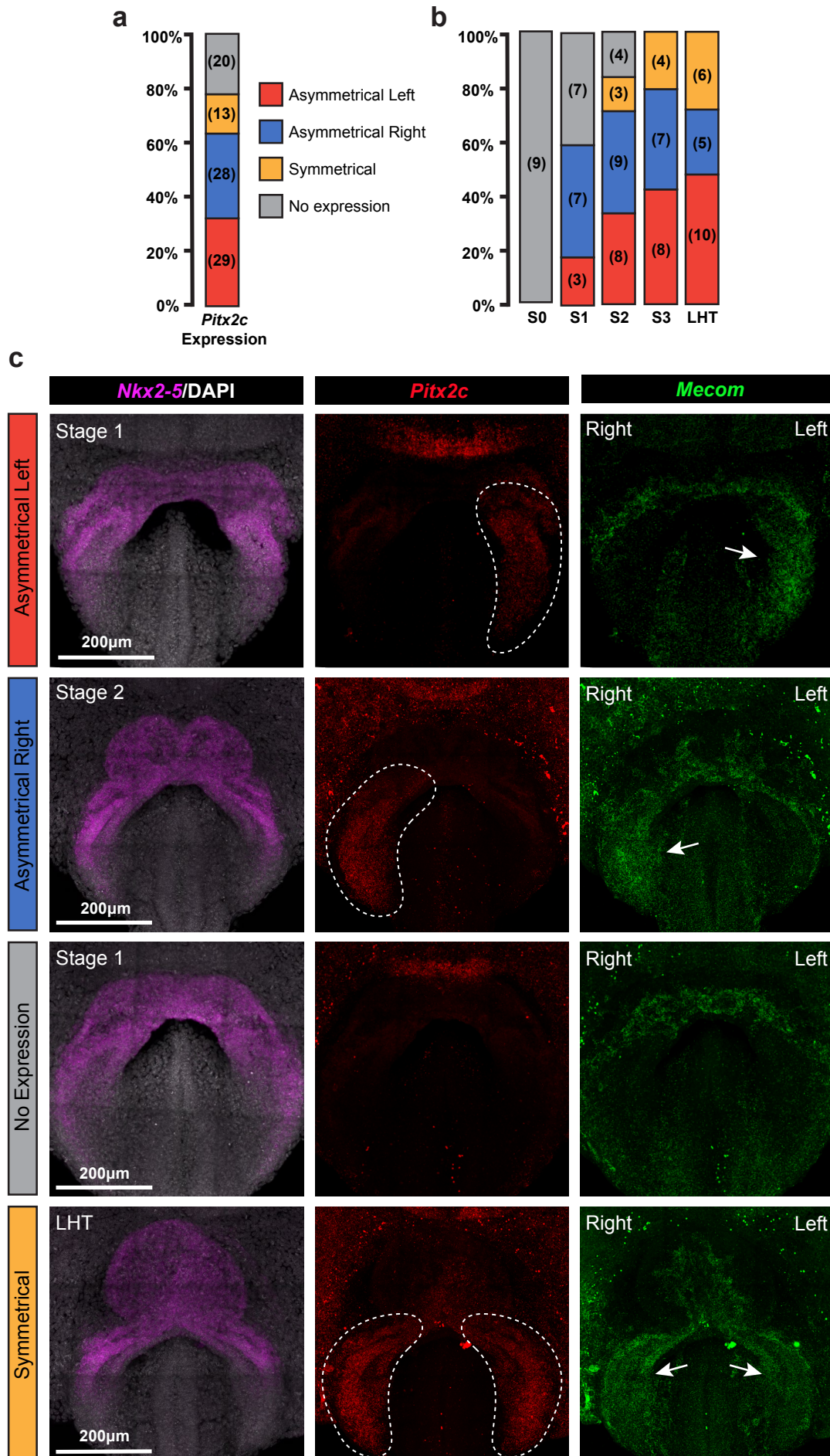
Figure 5: Characterization of Dnah11^iv/iv mutant phenotypes and Mecom expression. a-b, Combined and stage-specific quantification of *Pitx2c* expression patterns in iv/iv mutant embryos during cardiac crescent development. Number of embryos shown in brackets. **c**, Maximum Intensity Projections (MIP) of hybridization chain reaction (HCR) staining revealing the expression pattern of *Mecom*, in embryos with different *Pitx2c* expression profiles. Dotted regions represent *Pitx2c* expression and arrows mark *Mecom* expression.

in the endothelium and LPM are independently regulated and that the asymmetric LPM expression is determined by the same mechanisms that control asymmetric *Pitx2c* expression.

DISCUSSION

Given the importance of left-right asymmetry in the formation of the body plan, it is fundamental to understand how these asymmetries arise during development. Our study characterizes the molecular differences which are present during symmetry breaking in the mouse embryo, specifically in the context of the embryonic heart, which is the first organ during development to manifest morphological indications of left-right asymmetry[18].

Having previously mapped and characterized the cell types present in the anterior heart forming region of the embryo, we used this dataset to identify asymmetrically expressed genes and validated their expression pattern using HCR. Overall left-right transcriptional differences were subtle, having no influence on cell clustering. However, due to our manual sub-dissection, we retained information about whether cells originate on the left or right sides of the cardiac crescent and could leverage this information to identify genes that were expressed with a left or right sided bias. The vast majority of asymmetrically expressed genes were identified within mesodermal cell populations, highlighting germ layer specific responses to symmetry breaking at the node. In contrast to previous attempts at identifying left-right asymmetric gene expression, that identified genes relating predominantly to cardiomyocyte differentiation[20], the asymmetric genes we have identified and validated play roles in a wide range of biological processes, highlighting the complexity by which asymmetry manifests. These include extracellular matrix remodeling (*Mmp9*), signaling (*Sema3a*), cell cycle progression (*Mecom*) and translation regulation (*Ybx3*). Apart from *Mmp9*, none of these genes have previously been implicated in left-right asymmetry breaking and therefore it would be important to further test and characterize the functional role of these genes in this process. Interestingly, homozygous Evi1 (*Mecom*) knockout mice die at around 10.5dpc. Mutant embryos had widespread hypocellularity and hemorrhaging, and hearts which had a more tube-like appearance, potentially suggesting a looping defect[30].

Given our previous high-fidelity mapping of cell types in the cardiac region of the embryo[21], we could also validate asymmetric gene expression biases within distinct anatomical locations. For example, *Mmp9* was most strongly expressed in cells from transcriptional clusters Me7, Me6, Me3 and endothelial cells (Me2). Anatomical validation of asymmetric *Mmp9* expression in the embryo showed expression in a specific region of the cardiac crescent which marked the transition from cardiac progenitors to cardiomyocytes (Figure S6b)[21]. This anatomical region transcriptionally represented cells from cluster Me6, which strongly expressed *Mmp9*, highlighting how this dataset can identify specific L/R asymmetries in transcriptionally and anatomically distinct populations of cells. Given the role of MMP9 in extracellular matrix remodeling it would suggest that this early asymmetric *Mmp9* expression plays a role in the onset of LHT looping.

Our computational analysis revealed several genes with right sided bias, which is striking given that relatively few right-asymmetric genes have been reported in the mouse embryo. Two such examples are *Cerl2*, whose transcripts are stabilized preferentially on the right side of the node; and *Snai1*, expressed more strongly in the right LPM than left[31–35]. When validating right-sided genes using HCR, we found a greater degree of variability in their expression patterns compared to left-sided genes. They did not always show right-sided expression, suggesting potential intrinsic differences in the regulation of right-sided genes compared to the left. This variability could reflect a less-stable, more transient, expression profile for right-sided gene expression relative to the left, which is robustly controlled by the node and downstream *Pitx2c* activation. Alternatively, it could reflect the overall high levels of expression of right sided genes in all cell types, resulting in a technical inability to detect relatively small or localized changes in gene expression levels.

One of the most significant right-sided genes was *Ybx3*, which encodes a DNA and RNA binding protein. YBX3 post-translationally controls mRNA stability and translation, having a role in the regulation of cell proliferation and density as well as in amino acid uptake[24,36]. Asymmetric proliferation rates have been reported to play a role in driving rightward looping of the LHT, with increased rates of proliferation of the right side of the venous pole[19,37]. Reduction of YBX3 in vitro leads to a decrease in proliferation, potentially highlighting that it may play a role in regulating asymmetric proliferation differences during early cardiac morphogenesis.

We have observed the spread of *Pitx2c* expression, from a distal region of LPM adjacent to the node, proximally through the LPM and into the cardiac crescent. In contrast we have observed the maintenance of symmetric *Pitx2c* expression in the head folds and yolk sac endoderm, highlighting tissue specific regulation of this gene. Interestingly, we discovered other genes which showed tissue specific asymmetries, such as *Mecom*. Prior to the asymmetric expression of *Pitx2c*, *Mecom* could be detected symmetrically in the endothelial cells of the presumptive endocardium. However, after *Pitx2c* became asymmetric, *Mecom* too became asymmetrically expressed in the LPM, while remaining symmetrically expressed in the endocardium. This highlights differences in the regulation of asymmetric genes within similar anatomical regions but in a cell type specific manner (i.e. endothelial vs. LPM) and could reflect how asymmetric signals propagate from the node but also how these different cell types respond to the asymmetry generating signals. It also indicates that within the heart, different cell types contribute disproportionately to the generation of morphological asymmetries.

This study represents a comprehensive transcriptional characterization of asymmetry breaking during cardiac crescent development, in the framework of a single-cell dataset. Given the central role left-right asymmetry plays in cardiac morphogenesis, it provides a valuable resource for further mechanistic studies, aiding in our understanding of congenital heart diseases.

MATERIALS AND METHODS

Mouse strains, husbandry and embryo collection

All animal experiments complied with the UK Animals (Scientific Procedures) Act 1986, approved by the local Biological Services Ethical Review Process and were performed under UK Home Office project licenses PPL 30/3420 and PCB8EF1B4. To obtain wild-type embryos, C57BL/6 males (in house) were crossed with 8-16 week old CD1 females (Charles River, England). All mice were maintained in a 12-hr light-dark cycle. Noon of the day when a vaginal plug was found was designated E0.5. To dissect the embryos, the pregnant females were culled by cervical dislocation in accordance with schedule one of the Animals (Scientific Procedures) Act. Embryos of the appropriate stage were dissected in M2 medium (Sigma-Aldrich, Cat No. M7167).

Dissection and unbiased collection of cells from the mouse cardiac crescent

Following dissection, embryos were collected, keeping the yolk sac intact, in fresh M2 media before being grouped based on their cardiac crescent stage**.** Progressive crescent stages (-1 to 3) were defined based on morphological criteria including the shape of the cardiac crescent and the ratio between width (medio-lateral axis) and maximum height (rostral-caudal axis) of the crescent[38]. Stage -1 embryos were defined based on the incomplete fusion of the mesodermal wings in the anterior portion of the embryo. Embryos were considered to be at the LHT stage once both sides of the cardiac crescent were completely folded and fused. Embryos prior to cardiac crescent formation were staged using the Lawson and Wilson staging system of mouse development[39].

Once embryos were staged, crescent regions were micro-dissected using tungsten needles, keeping the overlying endoderm intact. By maintaining the integrity of the overlying endoderm at cardiac crescent and LHT stages, regions of both yolk sac endoderm and embryonic endoderm were also collected as well as the forming pericardium. To isolate cardiac crescent regions, the anterior half of the embryo was dissected from the posterior before a cut was made along the midline separating the embryo into left and right sides. The cardiac crescent could then be isolated using the sagittal profile to collect both dorsal and ventral tissue. Left and right sides of the sub-dissected regions where disaggregated and processed separately. At LHT stage the heart tube was isolated by dissections from the ventral surface, due to both the morphology and size of the tissue, therefore it is unlikely we collected regions of the dorsal pericardial wall. Following isolation of the cardiac crescent region the tissue was pooled from multiple embryos (Embryos pooled: stage LHT: 5, stage 3; 7, stage 2; 27, stage 1; 18, stage 0; 7, stage -1; 2). The pooled samples were dissociated into single cells using 200µl Accutase (ThermoFisher, Cat No. A1110501) for 12 minutes at 37°C, being agitated every 2 minutes, before adding 200µl heat-inactivated FBS (ThermoFisher, Cat No. 10500) to quench the reaction. Cells were then centrifuged at 1000rpm for 3 minutes at 4°C before being suspended in 100µl HBSS (ThermoFisher, Cat No. 14025) + 1% FBS, and stored on ice. Single cells were collected using a Sony SH800 FACS machine with a stringent single-cell collection protocol and sorted into 384 well plates containing SMART-seq2 lysis buffer[40] plus ERCC spike-ins. To ensure we collected good quality cells, a live/dead dye (Abcam, Cat No. ab115347) was used; 100µl was added to the cell suspension at a 2x concentration in HBSS 10 minutes before collection, and live cells were collected based on their FITC intensity. Once cells were collected, plates were sealed, spun down, and frozen using dry ice before being stored at -80°C. This complete process, from dissection to single-cell collection, took approximately 2-3 hours. Cells were collected in multiple batches.

Differential expression analysis

To identify asymmetrically expressed genes, we used the previously reported data from Tyser et al, 2021, obtained from https://content.cruk.cam.ac.uk/jmlab/mouseEmbryonicHeartAtlas/. Briefly, single-cell transcriptomic data for good-quality cells is available in a SingleCellExperiment object (sce_goodQual.NORM.clusters.Rds), containing raw and normalized counts, together with batch, stage, side, and cluster annotations for each cell. This object was the basis for all analyses reported in this study.

To test for differential expression between cells from the left and right sides, we converted the SingleCellExperiment object into a DGElist object (convertTo function from scran package (Lun, McCarthy, Marioni, F1000Res, 2016)) to be used with edgeR (Robinson, McCarthy, Smyth, Bioinformatics, 2010). We analyzed each germ layer separately and used generalized linear models to test for differences between left and right sides in cells from each cluster (with glmQLFit and glmQLFTest), while controlling for batch (experiment date). Contrasts for all clusters from the same germ layer were tested together to reduce the number of tests performed; we thus obtained a single p-value indicating whether the gene is differentially expressed in *any* of the clusters tested (Me1 and Me2 were excluded due to their very small number of cells). P-values were adjusted for multiple testing using the Benjamini Hochberg method.

To define significant changes in expression, we required a gene to have an adjusted p-value smaller than 0.05 and an absolute fold-change larger than 1.5 for mesoderm clusters, and 1.3 for endoderm and ectoderm clusters. We filtered out genes with unstable fold-changes that stem from outlier expression in a small number of cells. For this, we computed the average gene expression levels in each cluster and ignored fold-change estimates from clusters where gene expression was lower than 1 normalized $\log_2$ count. We filtered out any genes that no longer fulfilled the minimum fold-change threshold from our list of significant results. This procedure ensures that the asymmetrically expressed genes defined are supported by at least moderate expression levels in the clusters showing differential expression. Full differential expression results are provided in Supplementary Table 2; fold-change estimates for clusters with very low expression are set to NA.

Cell-cycle phase differences

To test whether there are significant differences in the proportions of cells in non-cycling (G1) versus cycling (S and G2/M) cells between the left and right sides, we used a binomial test (with the proportions on the left used as the expected probabilities, and testing whether the proportions on the right were significantly different). Cell-cycle phase

assignment for each cell was originally inferred using Cyclone (Scialdone et al., 2015).

Whole mount immunostaining

Dissected intact embryos were fixed for 1 hr at room temperature with 4% paraformaldehyde (SantaCruz, Cat No. sc281692) in PBS (Sigma-Aldrich, Cat No. P4417). The embryos were then rinsed twice in PBST-0.1% (PBS with 0.1% Triton X-100 (Sigma-Aldrich, Cat No. T8787)) before being permeabilized in PBST-0.25% for 40 mins and rinsed again 3x in PBT-0.1%. The embryos were next transferred to blocking solution (5% donkey serum (Sigma-Aldrich, Cat No. D9663), 1%BSA (Sigma-Aldrich, Cat No. A7906) in PBST-0.1%) overnight (o/n) at 4°C. Primary antibodies (Goat Nkx2-5, Santa Cruz) were then added to the solution and were incubated o/n at 4°C. The embryos were washed 3x 15mins in PBST-0.1% and incubated o/n at 4°C in PBST-0.1% with the secondary antibodies, and DAPI, then subsequently washed 3x PBT-0.1% for 15 min and placed in Vectashield mounting medium with DAPI (Vector Labs, Cat No. H-1200) for at least 24 hr at 4°C. Each staining combination was repeated on at least 3 embryos. Samples were imaged using a Zeiss 880 confocal microscope with a 40x oil (1.36 NA) objective. Images were captured at 512 × 512 pixel dimension using multiple tiles with a Z-step of between 1.5 and 0.5 µm. Based on the working distance of the Zeiss 880 microscope and tissue penetration, embryos were imaged to a depth of between 120 – 150µm.

In Situ Hybridization Chain reaction (HCR)

In situ HCR kit (ver.3) containing amplifier set, hybridization, amplification, wash buffers, and DNA probe sets, were purchased from Molecular Instruments (molecularinstruments.org) and the protocol described in Choi et al. (2018) was followed with slight modifications[41]. Embryos were collected as previously described and fixed overnight in 4% paraformaldehyde at 4°C with shaking. Following fixation, the embryos were kept on ice and washed twice in cold nuclease free 0.1% PBS Tween (nucPBST) before being dehydrated in methanol with a series of graded MeOH/0.1% nucPBST washes (25% MeOH/75% nucPBST; 50% MeOH/50% nucPBST; 75% MeOH/25% nucPBST; 2x 100% MeOH) for 10 minutes on ice before being stored at -20°c in 100% MeOH. For HCR staining, embryos were rehydrated with a series of graded MeOH/PBST washes for 10 minutes each on ice (75% MeOH/25% nucPBST; 50% MeOH/50% nucPBST; 25% MeOH/75% nucfree PBST; 100% nucPBST; 100% nucPBST at room temperature). After rehydration, embryos were treated with 10 µg/ml proteinase K solution for 5 minutes at room temperature, washed twice for 5 minutes with nucPBST, post-fixed with 4% paraformaldehyde for 20 minutes at room temperature, then washed three times with nucPBST for 5 minutes. Embryos were next pre-hybridized with 50% probe hybridization buffer/ 50% nucPBST at room temperature for two hours before being incubated with probe hybridization buffer for 30 minutes at 37°C prior to being incubated in probe solution (2 pmol of each probe in 500µl of 30% probe hybridization buffer) overnight (12-16 hours) at 37°C. Probe libraries were designed and manufactured by Molecular Instruments using *Mus musculus* sequences from NCBI database. Excess probe was removed by washing with pre-warmed probe wash buffer at 37°C four times for 15 minutes each and then two times 5 minutes with 5X SSCT buffer (5x

sodium chloride sodium citrate, 0.1% Tween 20 in ultrapure H2O). For amplification, embryos were incubated in amplification buffer for 30 minutes at room temperature before being placed into hairpin solution and incubated overnight in the dark at room temperature. 30 pmol hairpin solution was prepared by snap cooling (95°C for 90 seconds, then cooled to room temperature) stock hairpins in storage buffer and then diluted in amplification buffer at room temperature. Following overnight incubation, excess hairpins were removed by washing with 5X SSCT buffer at room temperature (2x 5 mins, 2x 30 mins with DAPI and 1x 5 min). Embryos were then placed into Vectashield antifade mounting medium (Vector Laboratories, Cat no. H-1000) or 87% glycerol solution, then imaged on a Zeiss 880 confocal microscope as previously described in the immunohistochemistry section. Each HCR combination was repeated on at least 3 embryos. Sagittal sections were generated using optical reconstruction of multiple Z-images.

REFERENCES

1. Little, R. B. & Norris, D. P. Right, left and cilia: How asymmetry is established. *Semin Cell Dev Biol* **110**, 11–18 (2021).

2. Collignon, J., Varlet, I. & Robertson, E. J. Relationship between asymmetric nodal expression and the direction of embryonic turning. *Nature 1996 381:6578* **381**, 155–158 (1996).

3. Lowe, L. A. *et al.* Conserved left–right asymmetry of nodal expression and alterations in murine situs inversus. *Nature 1996 381:6578* **381**, 158–161 (1996).

4. Nonaka, S. *et al.* Randomization of left-right asymmetry due to loss of nodal cilia generating leftward flow of extraembryonic fluid in mice lacking KIF3B motor protein. *Cell* **95**, 829–837 (1998).

5. Nonaka, S., Shiratori, H., Saijoh, Y. & Hamada, H. Determination of left–right patterning of the mouse embryo by artificial nodal flow. *Nature 2002 418:6893* **418**, 96–99 (2002).

6. Meno, C. *et al.* Left–right asymmetric expression of the TGFβ-family member lefty in mouse embryos. *Nature 1996 381:6578* **381**, 151–155 (1996).

7. Logan, M., Pagán-Westphal, S. M., Smith, D. M., Paganessi, L. & Tabin, C. J. The Transcription Factor Pitx2 Mediates Situs-Specific Morphogenesis in Response to Left-Right Asymmetric Signals. *Cell* **94**, 307–317 (1998).

8. Ryan, A. K. *et al.* Pitx2 determines left–right asymmetry of internal organs in vertebrates. *Nature 1998 394:6693* **394**, 545–551 (1998).

9. Yoshioka, H. *et al.* Pitx2, a bicoid-type homeobox gene, is involved in a lefty-signaling pathway in determination of left-right asymmetry. *Cell* **94**, 299–305 (1998).

10. Piedra, M. E., Icardo, J. M., Albajar, M., Rodriguez-Rey, J. C. & Ros, M. A. Pitx2 Participates in the Late Phase of the Pathway Controlling Left-Right Asymmetry. *Cell* **94**, 319–324 (1998).

11. Amand, T. R. S. *et al.* Cloning and expression pattern of chicken Pitx2: A new component in the SHH

signaling pathway controlling embryonic heart looping. *Biochem Biophys Res Commun* **247**, 100–105 (1998).

12. Kitamura, K. *et al.* Mouse Pitx2 deficiency leads to anomalies of the ventral body wall, heart, extra- and periocular mesoderm and right pulmonary isomerism. *Development* **126**, 5749–5758 (1999).

13. Schweickert, A., Campione, M., Steinbeisser, H. & Blum, M. Pitx2 isoforms: involvement of Pitx2c but not Pitx2a or Pitx2b in vertebrate left–right asymmetry. *Mech Dev* **90**, 41–51 (2000).

14. Franco, D. & Campione, M. The Role of Pitx2 during Cardiac Development: Linking Left–Right Signaling and Congenital Heart Diseases. *Trends Cardiovasc Med* **13**, 157–163 (2003).

15. Tyser, R. C. v *et al.* Calcium handling precedes cardiac differentiation to initiate the first heartbeat. *Elife* **5**, (2016).

16. Djenoune, L., Berg, K., Brueckner, M. & Yuan, S. A change of heart: new roles for cilia in cardiac development and disease. *Nature Reviews Cardiology 2021 19:4* **19**, 211–227 (2021).

17. Desgrange, A., le Garrec, J. F., Bernheim, S., Bønnelykke, T. H. & Meilhac, S. M. Transient Nodal Signaling in Left Precursors Coordinates Opposed Asymmetries Shaping the Heart Loop. *Dev Cell* **55**, 413-431.e6 (2020).

18. Esteban, I. *et al.* Pseudodynamic analysis of heart tube formation in the mouse reveals strong regional variability and early left–right asymmetry. *Nature Cardiovascular Research 2022 1:5* **1**, 504–517 (2022).

19. le Garrec, J. F. *et al.* A predictive model of asymmetric morphogenesis from 3D reconstructions of mouse heart looping dynamics. *Elife* **6**, (2017).

20. Behrens, A. N. *et al.* Nkx2-5 Mediates Differential Cardiac Differentiation Through Interaction with Hoxa10. *Stem Cells Dev* **22**, 2211 (2013).

21. Tyser, R. C. V. *et al.* Characterization of a common progenitor pool of the epicardium and myocardium. *Science* **371**, (2021).

22. Schweickert, A. *et al.* Left-asymmetric expression of Galanin in the linear heart tube of the mouse embryo is independent of the nodal co-receptor gene cryptic. *Dev Dyn* **237**, 3557–3564 (2008).

23. Lawson, K. A. & Wilson, V. A Revised Staging of Mouse Development Before Organogenesis. *Kaufman's Atlas of Mouse Development Supplement* Preprint at https://doi.org/10.1016/b978-0-12-800043-4.00003-8 (2016).

24. Amy Cooke, A. *et al.* The RNA-Binding Protein YBX3 Controls Amino Acid Levels by Regulating SLC mRNA Abundance SLC7A5 SLC3A2 Cell Reports The RNA-Binding Protein YBX3 Controls Amino Acid Levels by Regulating SLC mRNA Abundance. *Cell Rep* **27**, 3097–3106 (2019).

25. McGrath, J., Somlo, S., Makova, S., Tian, X. & Brueckner, M. Two populations of node monocilia initiate left-right asymmetry in the mouse. *Cell* **114**, 61–73 (2003).

26. Hummel, K. P. & Chapman, D. B. Visceral inversion and associated anomalies in the mouse. *Journal of Heredity* **50**, 9–13 (1959).

27. Layton, W. M. Random determination of a developmental process: Reversal of normal visceral asymmetry in the mouse. *Journal of Heredity* **67**, 336–338 (1976).

28. Supp, D. M., Witte, D. P., Steven Potter, S. & Brueckner, M. Mutation of an axonemal dynein affects left–right asymmetry in inversus viscerum mice. *Nature 1997 389:6654* **389**, 963–966 (1997).

29. Campione, M. *et al.* The homeobox gene Pitx2: mediator of asymmetric left-right signaling in vertebrate heart and gut looping. *Development* **126**, 1225–1234 (1999).

30. Hoyt, P. R. *et al.* The Evi1 proto-oncogene is required at midgestation for neural, heart, and paraxial mesenchyme development. *Mech Dev* **65**, 55–70 (1997).

31. Marques, S. *et al.* The activity of the Nodal antagonist Cerl-2 in the mouse node is required for correct L/R body axis. *Genes Dev* **18**, 2342–2347 (2004).

32. Nakamura, T. *et al.* Fluid flow and interlinked feedback loops establish left–right asymmetric decay of Cerl2 mRNA. *Nature Communications 2012 3:1* **3**, 1–13 (2012).

33. Sefton, M., Sánchez, S. & Nieto, M. A. Conserved and divergent roles for members of the Snail family of transcription factors in the chick and mouse embryo. *Development* **125**, 3111–3121 (1998).

34. Murray, S. A. & Gridley, T. Snail family genes are required for left-right asymmetry determination, but not neural crest formation, in mice. *Proc Natl Acad Sci U S A* **103**, 10300–10304 (2006).

35. Rago, L. *et al.* MicroRNAs Establish the Right-Handed Dominance of the Heart Laterality Pathway in Vertebrates. *Dev Cell* **51**, 446-459.e5 (2019).

36. Balda, M. S., Garrett, M. D. & Matter, K. The ZO-1–associated Y-box factor ZONAB regulates epithelial cell proliferation and cell density. *Journal of Cell Biology* **160**, 423–432 (2003).

37. Galli, D. *et al.* Atrial myocardium derives from the posterior region of the second heart field, which acquires left-right identity as Pitx2c is expressed. *Development* **135**, 1157–1167 (2008).

38. Tyser, R. C. V. *et al.* Calcium handling precedes cardiac differentiation to initiate the first heartbeat. *Elife* **5**, (2016).

39. Lawson, K. A. & Wilson, V. A Revised Staging of Mouse Development Before Organogenesis. in *Kaufman's Atlas of Mouse Development Supplement* (2016). doi:10.1016/b978-0-12-800043-4.00003-8.

40. Picelli, S. *et al.* Full-length RNA-seq from single cells using Smart-seq2. *Nat Protoc* (2014) doi:10.1038/nprot.2014.006.

41. Choi, H. M. T. *et al.* Third-generation in situ hybridization chain reaction: Multiplexed, quantitative,

sensitive, versatile, robust. *Development (Cambridge)* (2018) doi:10.1242/dev.165753.

AUTHOR CONTRIBUTIONS

DATA AND MATERIALS AVAILABILITY

This study utilizes previously reported data (Tyser, Ibarra-Soria et al, Science, 2021), obtained from https://content.cruk.cam.ac.uk/jmlab/mouseEmbryonicHeartAtlas/. All code used for data analysis and figure generation is available at https://github.com/MarioniLab/leftRight_asymmetry.

a

Cluster	Left	Right
Ec1	103	76
Ec2	61	28
En1	170	165
En2	106	122
Me1	9	35
Me2	28	23
Me3	328	315
Me4	116	91
Me5	162	177
Me6	39	18
Me7	256	186
Me8	58	33

b

c
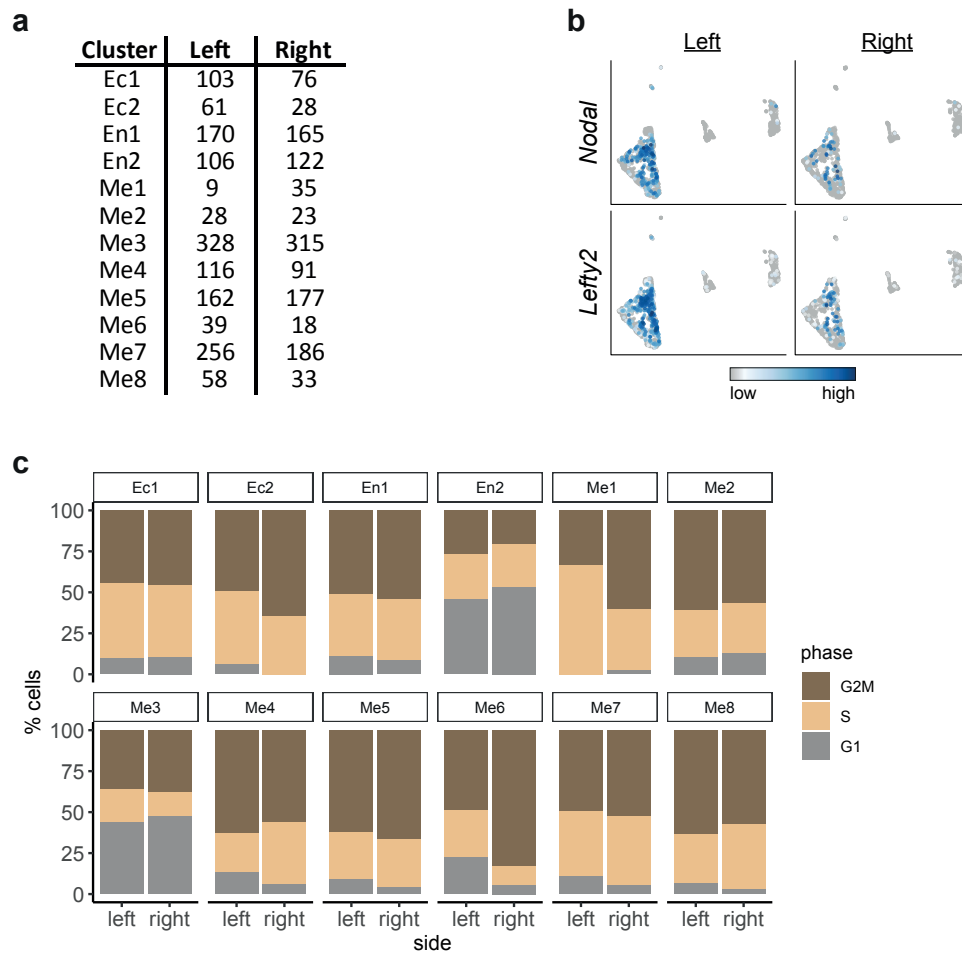
Figure S1: Characterization of left right differences during cardiac crescent development. **a**, Table showing the number of cells from each transcriptional cluster collected from either the left or right side of the embryo. **b**, UMAP showing the expression of Lefty2 and Nodal in cells collected from either the left or right side of the forming cardiac crescent. **c**, Bar graphs showing the proportion of left and right cells from different cell clusters in either G1, S or G2M phase of the cell cycle.

Gene	FDR	FC
Hnrnpab	9.74E-06	-0.473
Kif12	3.01E-05	-1.653
Ybx1	1.22E-04	-0.403
4930526A20Rik	1.73E-04	1.158
Cdkn1a	7.49E-04	-1.626
Proc	7.49E-04	-1.494
Apob	8.00E-04	-0.717
Eif3b	1.44E-03	-0.571
Gm13050	2.49E-03	0.760
Bag1	3.59E-03	-0.444
Gatad1	5.46E-03	-0.550
Stc1	5.63E-03	1.693
Prkaca	1.09E-02	-0.572
Polr2a	1.21E-02	-0.567
Polr2g	1.22E-02	-0.428

Gene	FDR	FC
Chrna4	5.49E-06	3.044
Fam69c	5.55E-04	-0.912
Olfml3	5.55E-04	-2.584
Timp3	7.41E-04	-2.065
Plac8	8.22E-04	-2.942
Rfx4	8.80E-04	-1.276
RP23-337L12.6	8.80E-04	-0.917
Gm14450	1.79E-03	0.651
Fezf1	2.19E-03	-1.839
Six3os1	2.54E-03	1.867
Fam195a	4.43E-03	3.469
Cnn3	5.68E-03	-0.544
Abhd11os	6.46E-03	2.884
Gm6655	6.46E-03	-1.054
Gm13904	7.18E-03	1.137

Figure S2: Identification of asymmetrically expressed genes in the endoderm and ectoderm. Differential expression analysis in the endodermal (**a**) and ectodermal (**b**) cells. The adjusted p-value (y-axis) is plotted against the fold-change between left-right cells (x-axis). For non-differentially expressed genes (grey), the average fold-change for all clusters is used; for DEGs (red) the largest fold-change (in clusters where the gene is expressed) is used. Genes are considered DE if their adjusted p-value is lower than 0.05 and their fold-change is larger than 1.3 (indicated by the dashed lines). Tables below show the top 15 DEGs, along with false discovery rate (FDR) and log fold change (FC) when comparing cells collected from either the left or the right.
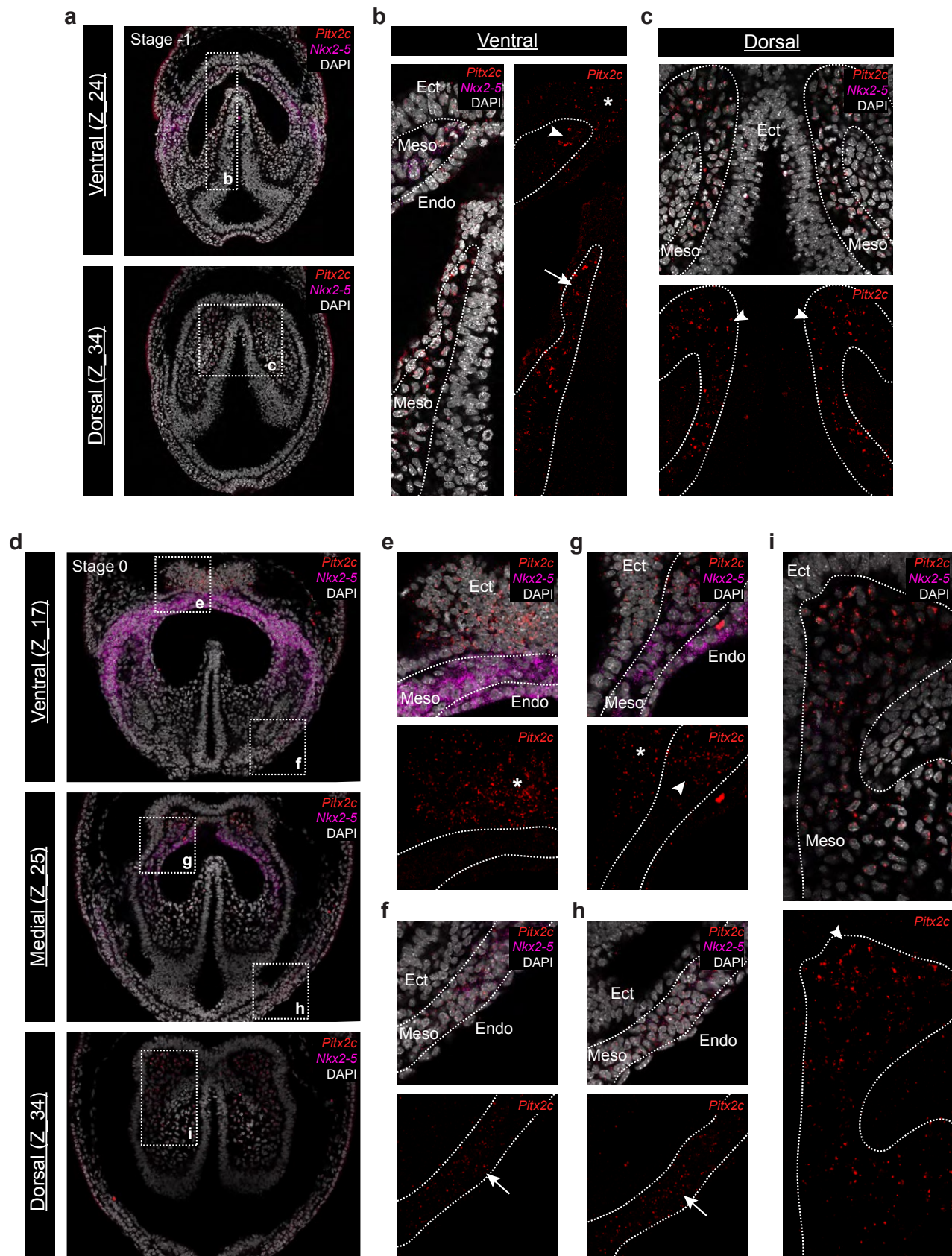
Figure S3: Detailed tissue specific characterization of Pitx2c expression during the onset of symmetry breaking. a, Individual ventral (top) and dorsal (bottom) sections of hybridization chain reaction (HCR) staining revealing the expression pattern of *Pitx2c* and *Nkx2-5* in a stage -1 cardiac crescent embryo (Figure 2a). **b**, Insert from panel a showing the ventral expression of *Pitx2c* in the paraxial (arrow) and cranial (arrowhead) mesoderm and neurectoderm (asterisks). Meso; mesoderm; Ecto, neuroectoderm; Endo, endoderm. **c**, Insert from panel a showing the dorsal expression of *Pitx2c* in the cranial mesoderm (arrowheads). **d**, Individual ventral (top), medial (middle) and dorsal (bottom) sections of hybridization chain reaction (HCR) staining revealing the expression pattern of *Pitx2c* and *Nkx2-5* in a stage 0 cardiac crescent embryo (Figure 2a). **e**, Insert from panel d showing the ventral expression of *Pitx2c* in the neurectoderm (asterisks). **f**, Insert from panel d showing the ventral expression of *Pitx2c* in the left distal lateral plate mesoderm (arrow). **g**, Insert from panel d showing the medial expression of *Pitx2c* in the cranial mesoderm (arrowheads) and neurectoderm (asterisks). **h**, Insert from panel d showing the medial expression of *Pitx2c* in the left distal lateral plate mesoderm (arrow). **i**, Insert from panel d showing the expression of *Pitx2c* in the dorsal cranial mesoderm (arrowhead).
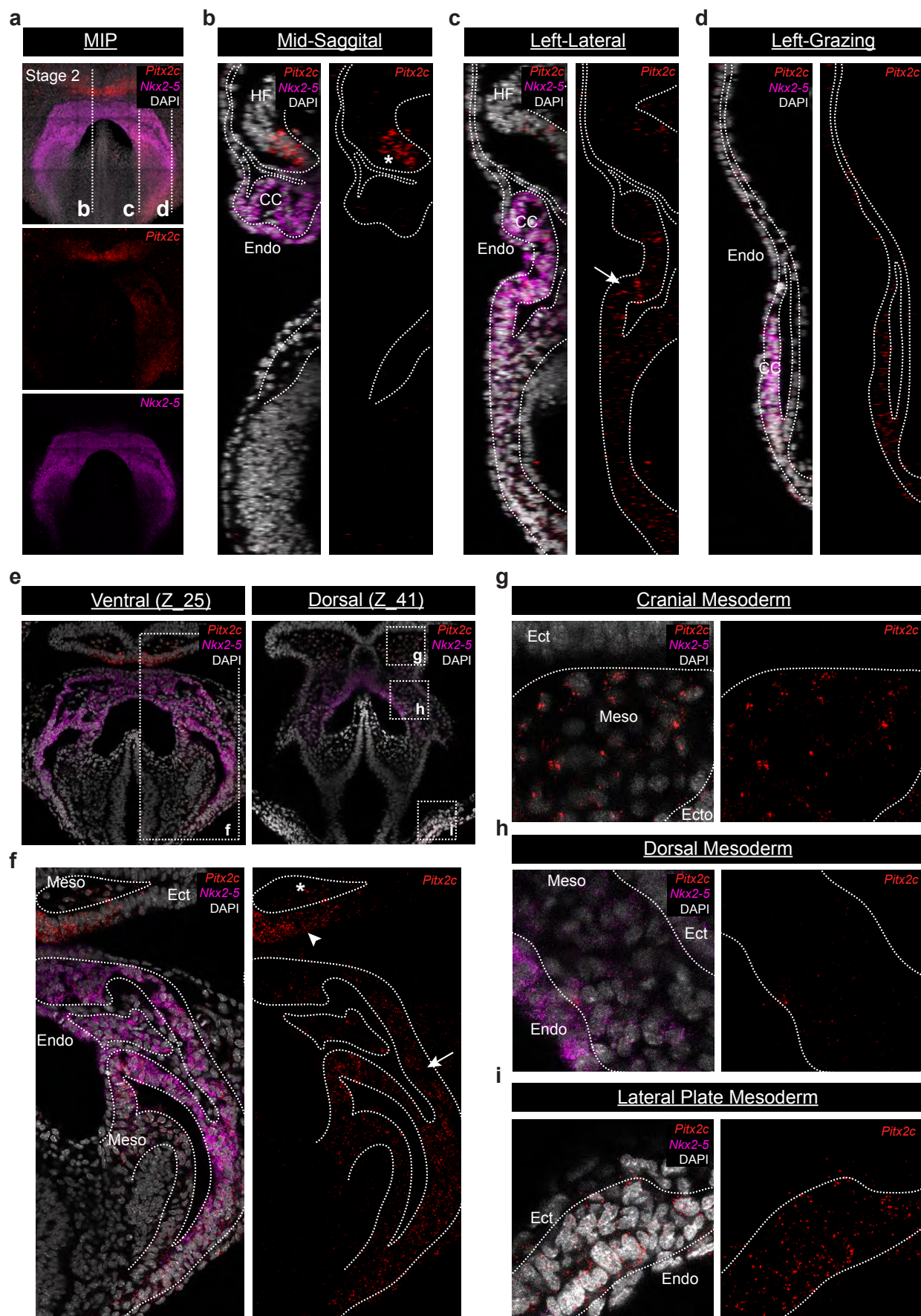
Figure S4: Expression pattern of Pitx2c in a stage 2 cardiac crescent. a, Maximum intensity projection (MIP) of a stage 2 cardiac crescent embryo showing expression of *Nkx2-5* and *Pitx2c* using Hybridization Chain Reaction (HCR). **b**, Mid-sagittal section of the embryo in panel a, showing expression of *Pitx2c* in neurectoderm (asterisks) and absence from the cardiac crescent (CC). Endo, endoderm; HF, headfold. **c**, Left-lateral section of the embryo in panel a, showing expression of *Pitx2c* in left lateral plate mesoderm and extending into the cardiac crescent (arrow). **d**, Left-grazing section of the embryo in panel a, showing expression of *Pitx2c* in distal left lateral plate mesoderm. **e**, Individual ventral (left) and dorsal (right) coronal sections of HCR staining from shown in figure S4a. **f**, Insert from panel e showing the ventral expression of *Pitx2c* in the left lateral plate mesoderm (arrows), cranial mesoderm (arrowheads) and neurectoderm (asterisks). Ect, ectoderm. **g**, **h**, **i**, Inserts from panel e showing the dorsal expresvsion pattern of *Pitx2c* in different left-sided mesoderm regions.
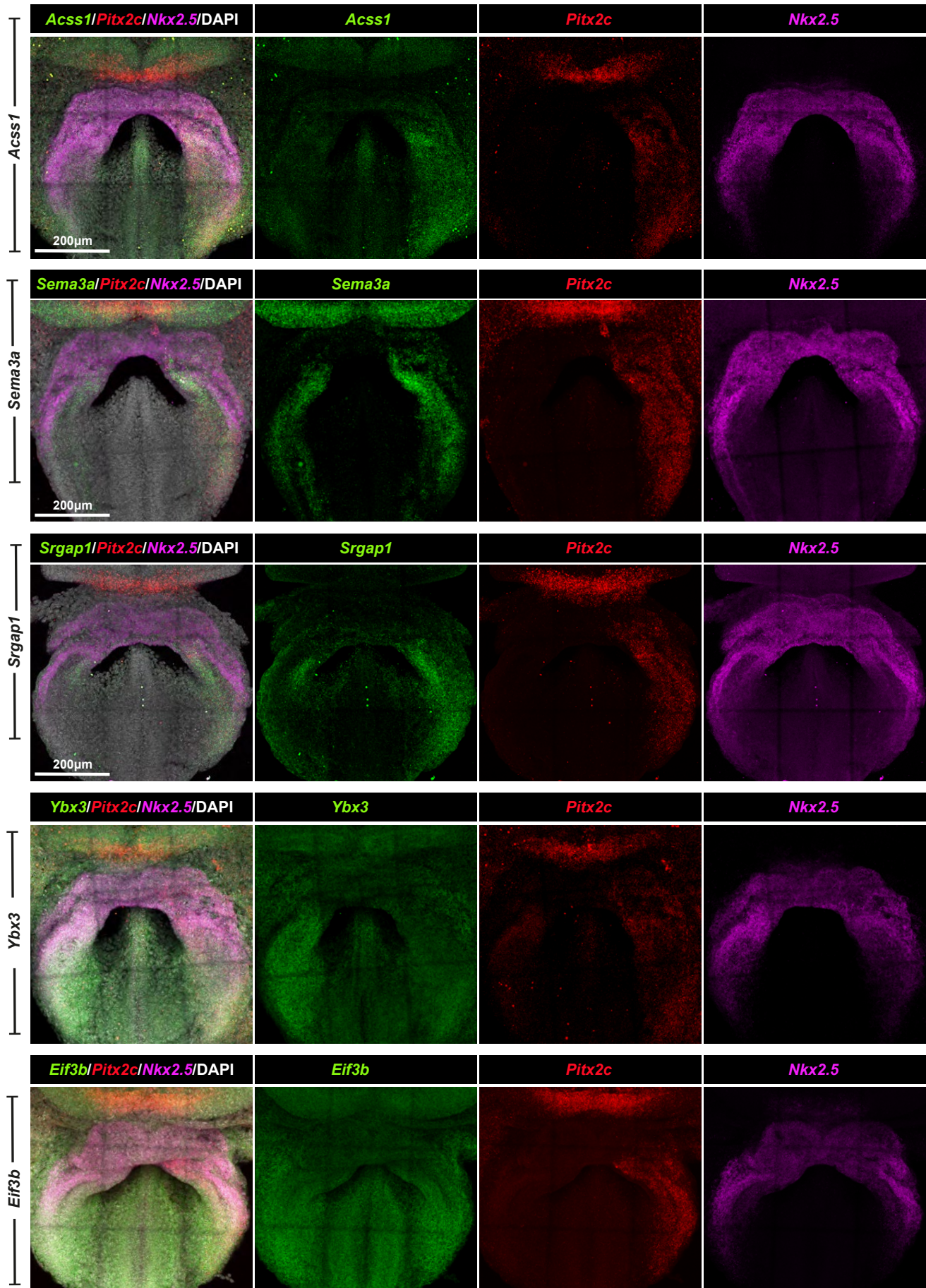
Figure S5: Individual channels for images in Figure 2. Maximum intensity projection (MIP) of a stage 2 cardiac crescent embryo showing expression of *Nkx2-5* and *Pitx2c* using Maximum Intensity Projections (MIP) showing merged and individual channels of hybridization chain reaction (HCR) staining from Figure 2c'-f'.

a

b
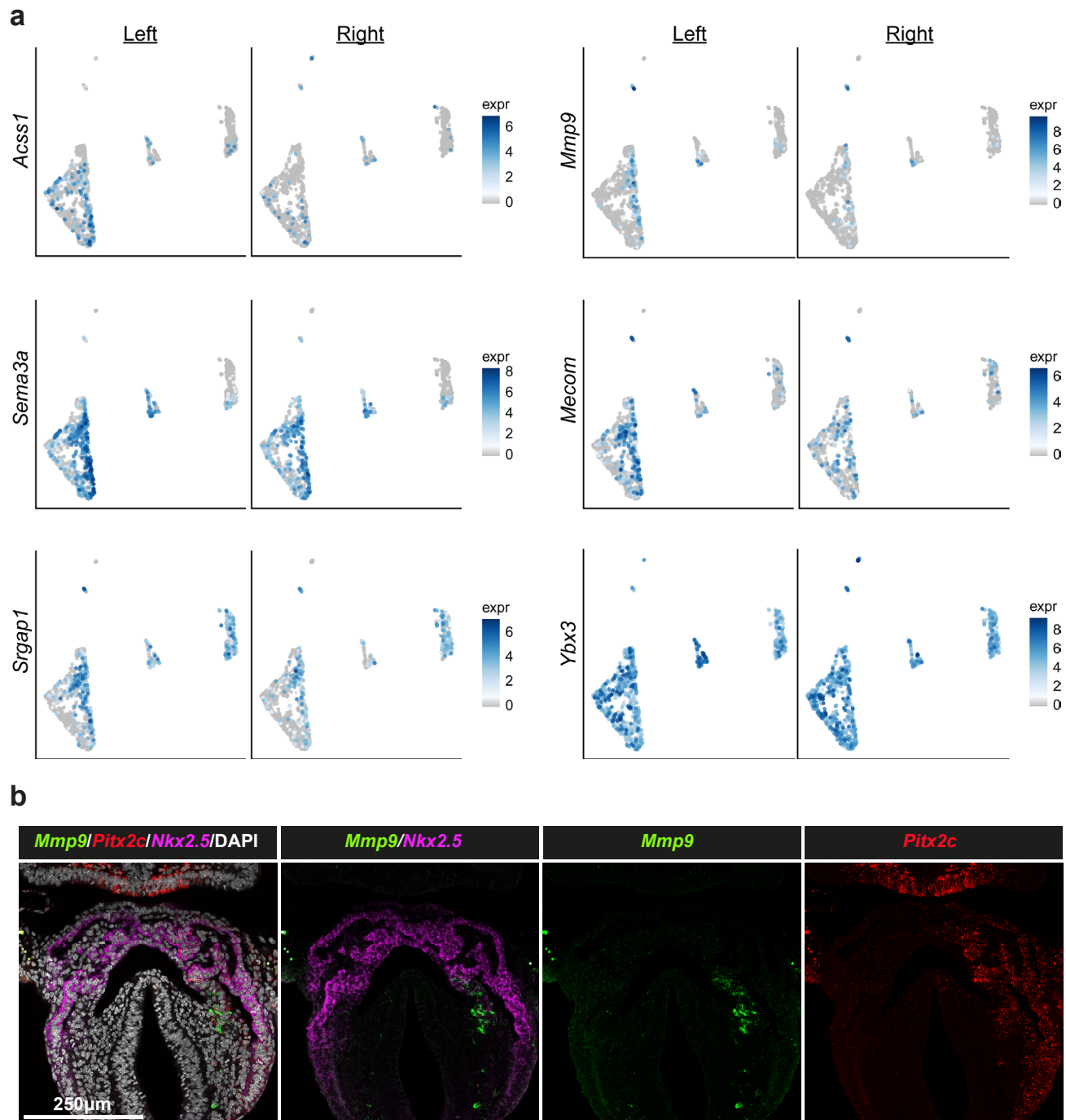
Figure S6: Asymmetric Mmp9 mesoderm is located in a distinct anatomical region of the developing cardiac crescent. a, UMAP showing the expression of *Acss1*, *Mmp9*, *Mecom*, *Srgap*, *Sema3a*, and *Ybx3* in cells collected from either the left or right side of the forming cardiac crescent. b, Individual sections from Figure 3e, showing the merged and separate expression pattern of *Mmp9*, *Pitx2c* and *Nkx2-5*.
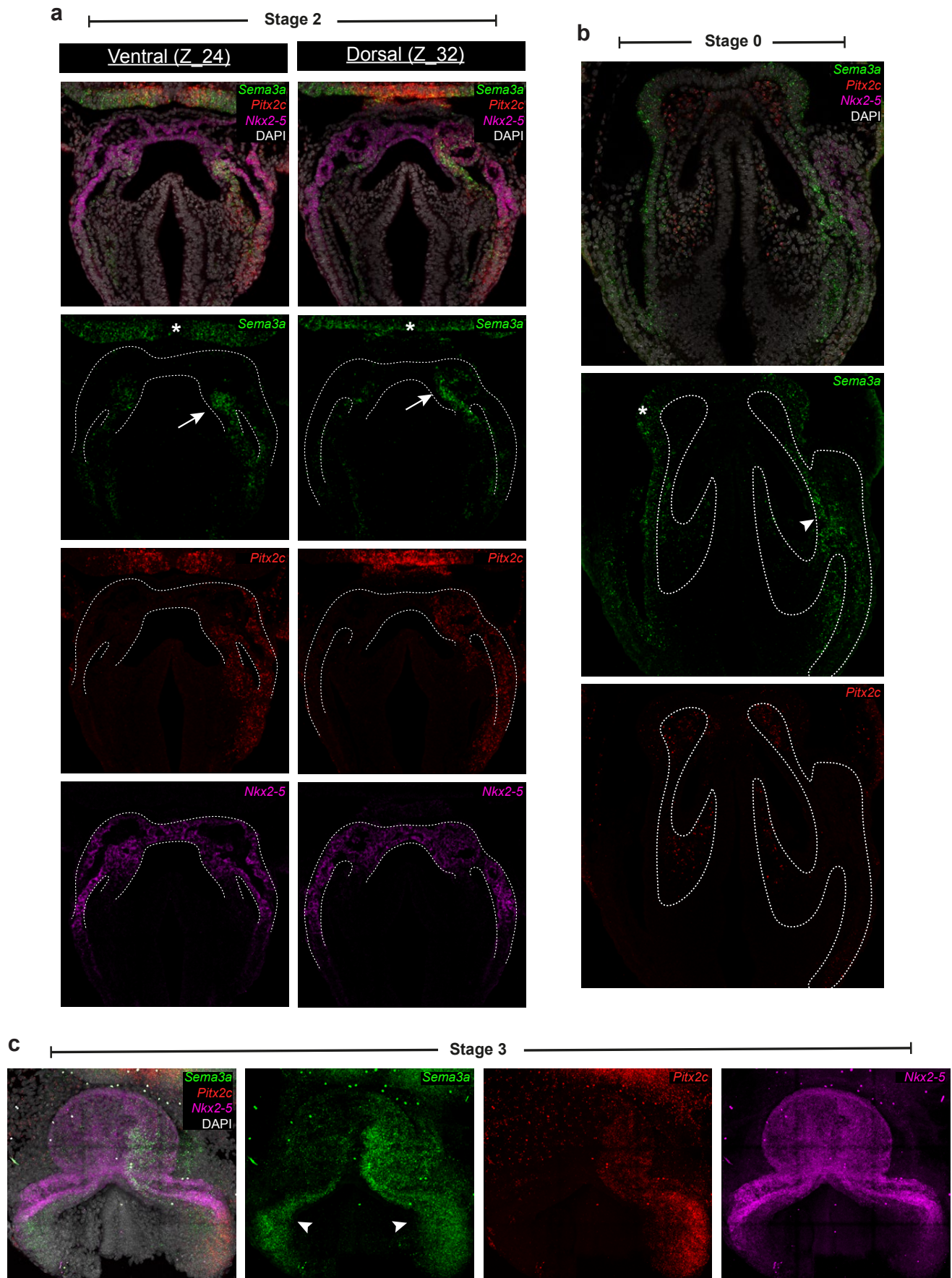
Figure S7: Expression of Sema3a in lateral plate mesoderm and neurectoderm. a, Ventral (left) and dorsal (right) Z sections showing hybridization chain reaction (HCR) staining for *Sema3a*, *Pitx2c* and *Nkx2-5* in a stage 2 cardiac crescent. Sema3a can be detected in both the neurectoderm (asterisks) as well as lateral plate mesoderm extending into the cardiac crescent (arrows). Dotted lines outline the cardiac crescent region. **b**, Z sections from Figure 4d showing hybridization chain reaction (HCR) staining for *Sema3a*, *Pitx2c* and *Nkx2-5* in a stage 0 cardiac crescent. *Sema3a* can be detected in both the neurectoderm (asterisks) as well as lateral plate mesoderm (arrows). Dotted lines outline mesoderm. **c**, Maximum intensity projection (MIP) of a linear heart tube stage embryo showing expression of *Sema3a*, *Nkx2-5* and *Pitx2c* using HCR. *Sema3a* expression extends throughout the left side of the heart tube but is also expressed in both venous poles (arrowheads).

Supplementary Table 1: Number of left/right cells detected in different cell-cycle phases.

Left

Cluster	Cell Number			Percentage		
	G1	G2M	S	G1	G2M	S
Ec1	10	46	47	9.7	44.7	45.6
Ec2	4	30	27	6.6	49.2	44.3
En1	19	87	64	11.2	51.2	37.6
En2	49	28	29	46.2	26.4	27.4
Me1	0	3	6	0.0	33.3	66.7
Me2	3	17	8	10.7	60.7	28.6
Me3	145	117	66	44.2	35.7	20.1
Me4	16	73	27	13.8	62.9	23.3
Me5	15	101	46	9.3	62.3	28.4
Me6	9	19	11	23.1	48.7	28.2
Me7	29	127	100	11.3	49.6	39.1
Me8	4	37	17	6.9	63.8	29.3

Right

Cluster	Cell Number			Percentage		
	G1	G2M	S	G1	G2M	S
Ec1	8	35	33	10.5	46.1	43.4
Ec2	0	18	10	0.0	64.3	35.7
En1	15	89	61	9.1	53.9	37.0
En2	65	25	32	53.3	20.5	26.2
Me1	1	21	13	2.9	60.0	37.1
Me2	3	13	7	13.0	56.5	30.4
Me3	151	118	46	47.9	37.5	14.6
Me4	6	51	34	6.6	56.0	37.4
Me5	8	118	51	4.5	66.7	28.8
Me6	1	15	2	5.6	83.3	11.1
Me7	11	97	78	5.9	52.2	41.9
Me8	1	19	13	3.0	57.6	39.4

Supplementary Table 2a: List of differentially expressed genes in left and right anterior endoderm. Results reported for all genes considered significantly differentially expressed. The fold-change in each cluster is reported. Clusters with very low expression were filtered out and the fold-change is NA. A summary fold-change is reported (**logFC**) and corresponds to the largest (absolute) fold-change from all clusters. Genes are considered significantly DE if FDR < 0.05 **AND** they show an absolute fold-change for at least one cluster larger than 1.3.

ensembl_ID	gene	logFC.En1	logFC.En2	logCPM	F	PValue	FDR	logFC
ENSMUSG00000020358	Hnrnpab	-0.472647531	-0.31376902	7.30176676	18.79626195	1.25E-08	9.74E-06	-0.472647531
ENSMUSG00000028357	Kif12	-1.652799735	-0.548600726	3.659703032	17.12161345	6.03E-08	3.01E-05	-1.652799735
ENSMUSG00000028639	Ybx1	-0.402535966	-0.32058833	9.526194112	15.347869	3.23E-07	0.000122097	-0.402535966
ENSMUSG00000085521	4930526A20Rik	1.157940904	-0.096023248	4.356331522	14.88794139	5.00E-07	0.000173181	1.157940904
ENSMUSG00000023067	Cdkn1a	-1.626392787	-1.026154439	4.821093968	12.89687639	3.33E-06	0.000749276	-1.626392787
ENSMUSG00000024386	Proc	-1.494186311	-0.470751487	3.112190371	12.87325662	3.41E-06	0.000749276	-1.494186311
ENSMUSG00000020609	Apob	NA	-0.716812183	4.841013442	12.76469794	3.78E-06	0.000799977	-0.716812183
ENSMUSG00000056076	Eif3b	-0.570886971	-0.44603501	7.928044041	12.05144335	7.49E-06	0.001437993	-0.570886971
ENSMUSG00000082575	Gm13050	0.759610663	0.107216593	5.728785136	11.26239195	1.60E-05	0.002492829	0.759610663
ENSMUSG00000028416	Bag1	-0.444170085	-0.356242694	6.77648054	10.80694979	2.48E-05	0.003594601	-0.444170085
ENSMUSG00000007415	Gatad1	-0.550357453	-0.288813809	5.979151133	10.26922297	4.16E-05	0.005464699	-0.550357453
ENSMUSG00000014813	Stc1	0.593908258	1.692700079	3.689396608	10.22675156	4.34E-05	0.005634022	1.692700079
ENSMUSG00000005469	Prkaca	-0.572472839	-0.342120015	6.021310139	9.457476083	9.12E-05	0.010937309	-0.572472839
ENSMUSG00000005198	Polr2a	-0.566619983	-0.240288525	6.351556104	9.342400262	0.000101915	0.012109418	-0.566619983
ENSMUSG00000071662	Polr2g	-0.428425071	-0.074094926	6.793318918	9.321134424	0.000104035	0.01219568	-0.428425071
ENSMUSG00000015575	Atp6v0e	-0.29215063	-0.400080229	7.059623576	8.728241246	0.000184801	0.018898148	-0.400080229
ENSMUSG00000110679	RP23-98C9.8	0.408282161	0.349909886	4.996825149	8.417922479	0.000249751	0.023391935	0.408282161
ENSMUSG00000068522	Aard	-1.159258316	0.924589916	4.365486147	8.264711366	0.000289827	0.025184887	-1.159258316
ENSMUSG00000015165	Hnrnpl	-0.386082881	-0.345389325	6.037360151	8.081789515	0.000346218	0.028417197	-0.386082881
ENSMUSG00000036242	3632451O06Rik	1.242279443	0.144561194	4.513648243	7.966431674	0.000387317	0.030975403	1.242279443
ENSMUSG00000040710	St8sia4	0.982628883	NA	3.586536407	7.882597726	0.000422374	0.032730049	0.982628883
ENSMUSG00000032083	Apoa1	-0.872789474	-1.494900438	7.659837709	7.822219969	0.000446512	0.03438693	-1.494900438
ENSMUSG00000068614	Actc1	-0.046025586	-1.285257665	4.860944065	7.479984719	0.000621885	0.043344363	-1.285257665

Supplementary Table 2b: List of differentially expressed genes in left and right anterior ectoderm. Results reported for all genes considered significantly differentially expressed. The fold-change in each cluster is reported. Clusters with very low expression were filtered out and the fold-change is NA. A summary fold-change is reported (**logFC**) and corresponds to the largest (absolute) fold-change from all clusters. Genes are considered significantly DE if FDR < 0.05 **AND** they show an absolute fold-change for at least one cluster larger than 1.3.

ensembl_ID	gene	logFC.Ec1	logFC.Ec2	logCPM	F	PValue	FDR	logFC
ENSMUSG00000027577	Chrna4	3.04425385	1.594869359	3.98322772	20.91805261	3.56E-09	5.49E-06	3.04425385
ENSMUSG00000047992	Fam69c	NA	-0.911888024	2.991565664	14.5699986	1.26E-06	0.000554811	-0.911888024
ENSMUSG00000027848	Olfml3	-2.584350871	-1.457605993	4.225379966	14.24214066	1.31E-06	0.000554811	-2.584350871
ENSMUSG00000020044	Timp3	-2.065135754	-1.987321244	3.594209768	13.77636558	2.00E-06	0.000740805	-2.065135754
ENSMUSG00000029322	Plac8	-1.457960881	-2.941957899	4.1726134	13.60995454	2.33E-06	0.000821769	-2.941957899
ENSMUSG00000020037	Rfx4	NA	-1.276295827	3.691202805	14.03319394	2.95E-06	0.000879534	-1.276295827
ENSMUSG00000111537	RP23-337L12.6	0.386841349	-0.916631318	4.669337762	13.63935191	2.99E-06	0.000879534	-0.916631318
ENSMUSG00000081661	Gm14450	-0.55669088	0.6514805	4.961172353	12.73751886	8.26E-06	0.001789057	0.6514805
ENSMUSG00000029697	Fezf1	NA	-1.838618801	3.601864696	12.6422984	1.05E-05	0.00219398	-1.838618801
ENSMUSG00000093460	Six3os1	1.86670429	-0.820241534	3.311407666	11.82048411	1.26E-05	0.002535732	1.86670429
ENSMUSG00000025732	Fam195a	0.622181572	3.468907287	3.997867045	10.91216855	2.77E-05	0.004434404	3.468907287
ENSMUSG00000053931	Cnn3	-0.446583198	-0.543603248	8.777816704	10.57711406	3.77E-05	0.005679904	-0.543603248
ENSMUSG00000085042	Abhd11os	-0.758654308	2.884309645	3.236447991	10.394856	4.47E-05	0.006462786	2.884309645
ENSMUSG00000107349	Gm6655	-0.598825661	-1.053787909	7.006827904	10.8118915	4.50E-05	0.006462786	-1.053787909
ENSMUSG00000082066	Gm13904	-0.013290674	1.136857999	7.080322176	10.55793616	5.41E-05	0.00718054	1.136857999
ENSMUSG00000004865	Srpk1	0.093220227	0.903887764	7.727567062	10.0603202	6.10E-05	0.008009336	0.903887764
ENSMUSG00000074280	Gm6166	0.492775681	1.082298693	7.553625453	9.737981337	8.24E-05	0.010358711	1.082298693
ENSMUSG00000082675	Gm6382	-0.478383449	-0.670888265	8.787777162	9.717382284	8.40E-05	0.010358711	-0.670888265
ENSMUSG00000031353	Rbbp7	-0.42325774	-0.619564754	9.223105908	9.706632451	8.48E-05	0.010358711	-0.619564754
ENSMUSG00000028480	Glipr2	-1.890637996	-1.829780076	4.37711213	9.686280042	8.64E-05	0.010358711	-1.890637996
ENSMUSG00000032128	Robo3	-2.162524589	-3.044199283	3.8201502	9.694268325	8.91E-05	0.010563405	-3.044199283
ENSMUSG00000051043	Gprc5c	0.38624706	-1.680446113	7.592589615	9.628890752	9.12E-05	0.010563405	-1.680446113
ENSMUSG00000031422	Morf4l2	-0.157285273	-0.7030003	9.021655446	9.604313474	9.33E-05	0.010566962	-0.7030003
ENSMUSG00000033227	Wnt6	-0.527682815	NA	6.100862779	9.508146576	0.000102095	0.011211576	-0.527682815
ENSMUSG00000009097	Tbx1	1.580826502	NA	5.348847792	9.470206914	0.000105781	0.011352549	1.580826502
ENSMUSG00000012282	Wnt8a	NA	-1.885250143	4.348658724	9.488221826	0.00010845	0.011440064	-1.885250143
ENSMUSG00000006586	Runx1t1	-1.080792568	NA	4.273354324	9.434174613	0.000109404	0.011442953	-1.080792568
ENSMUSG00000072235	Tuba1a	-0.3122222	-0.760776145	10.42307587	9.141601895	0.000143864	0.01411253	-0.760776145
ENSMUSG00000068748	Ptprz1	1.780122404	-0.897826246	4.186426703	9.141396441	0.000143892	0.01411253	1.780122404
ENSMUSG00000011114	Tbrg1	-0.314177067	-0.892497323	7.0803778	9.130753539	0.000145334	0.01411253	-0.892497323
ENSMUSG00000047721	Bola2	-0.09631218	1.634043075	5.78089499	9.114920051	0.000147506	0.01411253	1.634043075
ENSMUSG00000025508	Rplp2	0.071969213	1.288806923	8.031622136	9.000419973	0.000164219	0.014902832	1.288806923
ENSMUSG00000075334	Rprm	NA	1.547888973	3.00446825	11.42932996	0.000179517	0.01560284	1.547888973
ENSMUSG00000048001	Hes5	1.318449412	1.977880745	3.618776373	8.889757452	0.000182183	0.015723805	1.977880745
ENSMUSG00000083906	Gm15186	-0.596655118	0.593265839	4.114987246	8.908573778	0.000190379	0.016250292	-0.596655118
ENSMUSG00000057715	A830018L16Rik	1.30787139	2.673241468	3.595965882	8.773394027	0.000203214	0.017061697	2.673241468
ENSMUSG00000040659	Efhd2	-1.44655008	-1.899719937	4.371793993	8.743733377	0.000208956	0.0172909	-1.899719937
ENSMUSG00000004665	Cnn2	-0.852441163	-1.55114445	6.629582223	8.594639463	0.000240389	0.019126325	-1.55114445
ENSMUSG00000017723	Wfdc2	0.026702879	1.384502408	8.029533625	8.451580964	0.000275023	0.021214587	1.384502408
ENSMUSG00000031538	Plat	-0.054332687	-2.60392729	3.842252655	8.36002679	0.000299785	0.022155352	-2.60392729
ENSMUSG00000083856	Gm13886	0.086719952	0.864907167	4.316021872	8.320017511	0.000319484	0.023331777	0.864907167
ENSMUSG00000032178	Ilf3	0.107848332	0.720916822	8.450193483	8.12184205	0.000375254	0.026617165	0.720916822
ENSMUSG00000098761	Gm18821	0.266882334	0.952756115	6.759751697	8.138362558	0.000378756	0.026712029	0.952756115
ENSMUSG00000083700	Gm2986	-0.059042194	-1.356736008	6.189608406	17.2943399	0.000402608	0.028073356	-1.356736008
ENSMUSG00000039103	Nexn	-1.646060911	-0.769759287	3.496987266	7.980267113	0.000428909	0.029739268	-1.646060911
ENSMUSG00000100361	Gm7063	0.369047833	0.652878157	5.67914049	7.829535427	0.000524599	0.035188074	0.652878157
ENSMUSG00000080921	Rpl38-ps2	-0.062762885	1.177240831	7.850613963	7.732929652	0.000541875	0.036150393	1.177240831
ENSMUSG00000029718	Pcolce	-1.311221994	-2.495072471	3.623889674	7.707785125	0.000554921	0.036821688	-2.495072471
ENSMUSG00000010760	Phlda2	-1.484205642	-1.077416718	6.746988656	7.683856336	0.00056763	0.037463561	-1.484205642
ENSMUSG00000000078	Klf6	-1.065571264	-1.705862861	5.842185495	7.67043488	0.000574886	0.037474951	-1.705862861
ENSMUSG00000026180	Cxcr2	0.576383032	2.423248786	3.479297785	7.575265946	0.000629091	0.040258306	2.423248786
ENSMUSG00000101685	Gm17837	-0.04032279	0.620863755	5.001786457	7.530465298	0.000693277	0.043214251	0.620863755
ENSMUSG00000050856	Atp5k	-0.263750212	1.515470361	5.952928514	7.409901319	0.000735817	0.045407254	1.515470361
ENSMUSG00000027500	Stmn2	-1.60502667	-0.31950823	5.747772021	7.390994668	0.000749128	0.045770956	-1.60502667
ENSMUSG00000080893	Gm15920	-0.344563806	1.067682893	6.116167193	7.374620987	0.000760851	0.046258244	1.067682893
ENSMUSG00000041329	Atp1b2	-1.349242761	1.618019057	3.257736142	7.363324675	0.000769047	0.046409837	1.618019057
ENSMUSG00000022676	Snai2	-1.556790491	NA	4.260785306	7.368280327	0.000782656	0.046664435	-1.556790491
ENSMUSG00000056459	Zbtb25	-0.949630358	-2.314684896	4.296351883	7.319888038	0.000801398	0.047552168	-2.314684896
ENSMUSG00000058625	Gm17383	0.093722542	-0.656098608	7.801063554	7.314387307	0.000805591	0.047572283	-0.656098608
ENSMUSG00000040952	Rps19	0.247624843	0.859830346	8.481755057	7.300879064	0.000815983	0.047933104	0.859830346

Supplementary Table 2c: List of differentially expressed genes in left and right anterior mesoderm. Results reported for all genes considered significantly differentially expressed. The fold-change in each cluster is reported. Clusters with very low expression were filtered out and the fold-change is NA. A summary fold-change is reported (**logFC**) and corresponds to the largest (absolute) fold-change from all clusters. Genes are considered significantly DE if FDR < 0.05 **AND** they show an absolute fold-change for at least one cluster larger than 1.5.

ensembl_ID	gene	logFC.Me3	logFC.Me4	logFC.Me5	logFC.Me6	logFC.Me7	logFC.Me8	logCPM	F	PValue	FDR	logFC
ENSMUSG00000066652	Lefty2	2.84310673	1.37789794	5.75041157	2.53709154	2.54790275	-0.9180617	8.78141491	37.7076521	3.08E-43	1.86E-39	5.75041157
ENSMUSG00000027452	Acss1	1.42344536	1.30734274	1.81423214	3.21695947	2.66953694	NA	3.24633773	26.3256825	4.13E-30	1.00E-26	3.21695947
ENSMUSG00000027220	Syt13	-1.527319	NA	-1.9218108	2.75230836	1.11847012	0.70058174	3.46367053	23.7949989	3.42E-27	6.89E-24	2.75230836
ENSMUSG00000034037	Fgd5	1.37882211	-0.1770187	1.88311248	3.05017165	0.96171914	1.35047269	3.25666928	19.4891931	4.01E-22	6.92E-19	3.05017165
ENSMUSG00000017737	Mmp9	1.59736425	NA	NA	1.61076878	2.30583651	NA	3.37206631	19.1670984	9.62E-22	1.30E-18	2.30583651
ENSMUSG00000056076	Eif3b	-0.6475326	-0.8850013	-0.6818186	-0.2665037	-0.4898421	-0.3826226	7.94523159	19.1639692	9.70E-22	1.30E-18	-0.8850013
ENSMUSG00000028023	Pitx2	2.00363596	1.39299178	0.84345796	2.77811021	2.12671459	-0.6006121	6.00409557	17.9270032	2.84E-20	3.12E-17	2.77811021
ENSMUSG00000024907	Gal	1.99747282	-0.7151404	0.55956758	NA	1.8517723	NA	5.24208329	16.6131185	1.03E-18	8.27E-16	1.99747282
ENSMUSG00000067586	S1pr3	1.5166771	-0.1889733	1.24672003	NA	-0.685586	-0.7398197	3.31468789	14.8072248	1.42E-16	7.20E-14	1.5166771
ENSMUSG00000039630	Hnrnpu	-0.4071694	-0.6127353	-0.3476112	-0.3259561	-0.3059189	-0.3010718	9.0805614	14.3203224	5.31E-16	2.21E-13	-0.6127353
ENSMUSG00000038793	Lefty1	1.43910389	0.5085271	1.89250409	3.12600749	1.16133483	NA	3.63870938	14.0535995	1.10E-15	4.44E-13	3.12600749
ENSMUSG00000044186	Nkx2-6	-0.7969095	NA	-1.7104014	0.71573086	0.17025487	2.87289699	3.98515501	13.1703224	1.23E-14	4.13E-12	2.87289699
ENSMUSG00000015365	Mov10l1	-0.6448673	0.49487163	0.57161222	NA	NA	NA	4.29040452	12.0496191	2.65E-13	6.67E-11	-0.6448673
ENSMUSG00000030189	Ybx3	-0.6258284	-0.7644739	-0.3025733	-0.9350009	-0.3708768	-0.3999667	6.56776302	11.6474809	7.84E-13	1.86E-10	-0.9350009
ENSMUSG00000048387	Osr1	1.03570559	0.34768574	1.8027544	2.91169164	0.49860018	-1.8047221	4.22455205	11.2770722	2.15E-12	4.64E-10	2.91169164
ENSMUSG00000000690	Hoxb6	NA	NA	-1.0486938	NA	NA	NA	3.37712009	11.1308447	4.51E-12	8.80E-10	-1.0486938
ENSMUSG00000021381	Barx1	-0.6048359	NA	NA	NA	NA	NA	3.5463833	10.8430164	7.05E-12	1.28E-09	-0.6048359
ENSMUSG00000028072	Ntrk1	1.37740205	0.2180302	0.33781615	1.84451589	0.61687241	NA	3.31206919	10.8421491	7.09E-12	1.28E-09	1.84451589
ENSMUSG00000027624	Epb41l1	1.53562892	-0.318881	0.7399291	2.95359698	0.73676939	-0.7712605	3.67796923	10.5945727	1.38E-11	2.35E-09	2.95359698
ENSMUSG00000021506	Pitx1	NA	NA	1.01261747	NA	NA	NA	3.25784574	10.0091934	6.91E-11	1.09E-08	1.01261747
ENSMUSG00000032890	Rims3	-0.2998013	-0.4129602	1.77523609	0.34376775	-0.7086021	NA	4.982603	9.97713262	7.38E-11	1.14E-08	1.77523609
ENSMUSG00000023886	Smoc2	NA	-0.0131929	-0.6728728	NA	-0.0708888	-0.3566508	4.49788013	9.72482547	1.46E-10	2.16E-08	-0.6728728
ENSMUSG00000042401	Crtac1	0.64022639	0.13018587	1.5073025	2.14842348	1.30581207	-1.6001806	3.228771	9.66335247	1.73E-10	2.49E-08	2.14842348
ENSMUSG00000027684	Mecom	1.391631	-0.1008103	0.78106576	2.61596737	0.9846359	1.11778514	3.68507165	9.49300426	2.74E-10	3.81E-08	2.61596737
ENSMUSG00000036446	Lum	NA	NA	0.52675615	NA	NA	1.35060044	3.18217284	9.25709273	5.40E-10	7.18E-08	1.35060044
ENSMUSG00000013936	Myl2	-0.5558407	1.41635432	-1.8132091	-0.5864435	-1.0076283	NA	6.82952865	9.13643265	7.22E-10	9.49E-08	-1.8132091
ENSMUSG00000028883	Sema3a	1.22360838	0.17109158	0.9280138	0.70825621	0.57043747	0.80978186	5.70495372	9.0849937	8.28E-10	1.07E-07	1.22360838
ENSMUSG00000032911	Cspg4	1.03032048	1.99044019	-0.4865052	-0.293627	0.26770909	NA	3.42753263	9.00242965	1.05E-09	1.32E-07	1.99044019
ENSMUSG00000004415	Col26a1	-0.6788285	NA	0.51261059	2.62834651	0.47697535	0.58742601	4.20415743	8.93153804	1.25E-09	1.56E-07	2.62834651
ENSMUSG00000027230	Creb3l1	-0.1658976	-0.2043341	-1.0171822	NA	-1.4191681	-1.0866076	3.58229258	8.88950834	1.41E-09	1.72E-07	-1.4191681
ENSMUSG00000039782	Cpeb2	0.12119394	0.013412	0.25005492	-1.002992	0.95102713	NA	4.19021888	8.60363472	3.06E-09	3.39E-07	-1.002992
ENSMUSG00000037171	Nodal	1.22367553	1.11255501	1.66065847	1.80513521	1.51304225	NA	4.83925859	8.5617672	3.40E-09	3.69E-07	1.80513521
ENSMUSG00000020121	Srgap1	1.10437407	0.66257563	0.96789961	0.72323653	0.92670755	-0.3493411	3.63670205	8.25558071	7.77E-09	7.70E-07	1.10437407
ENSMUSG00000033161	Atp1a1	-0.3132229	-0.6500454	-0.4773622	-0.2046274	-0.3316488	-0.0673947	6.93379176	8.20004587	9.02E-09	8.80E-07	-0.6500454
ENSMUSG00000075304	Sp5	NA	NA	0.46003477	NA	0.44056347	-1.1995595	3.6959349	8.17153729	9.74E-09	9.35E-07	-1.1995595
ENSMUSG00000040694	Apobec2	0.42565255	0.13446034	0.49253268	1.05842841	1.35568302	NA	6.67291487	8.12625961	1.10E-08	1.05E-06	1.35568302
ENSMUSG00000070436	Serpinh1	0.13124918	-0.4680395	-0.5026817	0.9667432	0.18301809	2.25E-05	8.22407302	8.09572629	1.19E-08	1.11E-06	0.9667432
ENSMUSG00000005198	Polr2a	0.07930635	-0.7461497	-0.558627	0.83008439	-0.372487	-0.1272423	6.10015715	8.01764453	1.47E-08	1.35E-06	0.83008439
ENSMUSG00000059325	Hopx	-0.7373518	0.59915523	NA	-1.6818065	0.09294918	NA	3.10949852	7.90536927	2.13E-08	1.91E-06	-1.6818065
ENSMUSG00000031972	Acta1	0.14804934	1.0456274	-0.9316012	0.82465873	1.60126766	0.72355062	9.90558766	7.82063192	2.51E-08	2.23E-06	1.60126766
ENSMUSG00000079037	Prnp	0.50103812	0.22186438	-0.5648958	1.46724652	0.82343781	-0.0894837	6.66454931	7.71770349	3.30E-08	2.83E-06	1.46724652
ENSMUSG00000049532	Tecrl	0.52514998	-0.8155574	-0.6671055	-1.6363594	-0.8692927	NA	3.80626256	7.57280943	4.86E-08	4.00E-06	-1.6363594
ENSMUSG00000026837	Col5a1	0.47306722	0.41709851	0.0932287	1.40022654	0.97250038	1.19691377	5.36968042	7.38508871	8.04E-08	6.08E-06	1.40022654
ENSMUSG00000013584	Aldh1a2	1.07381431	0.22598676	0.36143821	-0.4423041	-0.4984436	-2.7504846	6.36362619	7.27988388	1.07E-07	7.86E-06	-2.7504846
ENSMUSG00000049422	Chchd10	-0.167829	-0.4715328	1.55413297	2.1219447	-0.0023699	NA	4.71578517	7.20650662	1.30E-07	9.07E-06	2.1219447
ENSMUSG00000038352	Arl5c	0.28077307	2.01516633	1.11715373	1.94955879	0.64116705	0.07137383	3.93130017	7.16366222	1.45E-07	1.01E-05	2.01516633
ENSMUSG00000051339	2900026A02R	-0.0119667	0.2176532	1.38815059	2.32039994	0.8800082	NA	4.21527526	7.03082638	2.07E-07	1.41E-05	2.32039994
ENSMUSG00000022103	Gfra2	0.52779673	2.3224927	-0.9039773	0.61988335	0.47258525	-0.7731323	3.84589394	6.88174868	3.08E-07	2.00E-05	2.3224927
ENSMUSG00000025647	Shisa5	0.76386243	0.22628905	0.33798741	0.91422725	0.61434241	0.58793095	6.0238678	6.75818426	4.28E-07	2.63E-05	0.91422725
ENSMUSG00000081677	Mdk-ps1	-0.159605	-0.9925873	-0.0186456	NA	0.20127991	-0.2136516	4.95407969	6.70416789	4.95E-07	3.02E-05	-0.9925873
ENSMUSG00000040666	Sh3bgr	0.04594873	0.27423067	-0.0322478	0.81894235	0.99316799	NA	7.64169825	6.66623521	5.47E-07	3.29E-05	0.99316799
ENSMUSG00000034486	Gbx2	NA	NA	NA	NA	0.12905224	1.20960757	3.24861511	6.53323255	7.85E-07	4.58E-05	1.20960757
ENSMUSG00000025597	Klhl4	-0.1391783	NA	0.66113994	0.6445112	0.25546516	NA	3.28344165	6.31380165	1.39E-06	7.70E-05	0.66113994
ENSMUSG00000051123	Cacna1c	0.1828239	0.80734197	1.01225731	1.7804778	0.59115773	NA	4.77732369	6.29501193	1.46E-06	7.96E-05	1.7804778
ENSMUSG00000021747	4930452B06R	0.88742621	0.35306126	0.41759887	0.88244797	1.04482729	-0.5541895	4.49934087	6.28975602	1.48E-06	7.99E-05	1.04482729
ENSMUSG00000041836	Ptpre	-0.3508813	-0.2386583	-1.0388508	-0.6493793	-0.0285948	NA	4.07340272	6.09961853	2.45E-06	0.00012621	-1.0388508
ENSMUSG00000042436	Mfap4	0.61251363	0.72161054	1.11801581	0.76251058	0.71342488	0.23622718	5.04909759	6.0651307	2.68E-06	0.00013475	1.11801581
ENSMUSG00000024500	Ppp2r2b	NA	NA	1.1728108	NA	0.39488014	NA	2.99529298	6.06595446	2.69E-06	0.00013471	1.1728108
ENSMUSG00000026586	Prrx1	0.63657229	1.14568046	0.82611365	NA	0.14327263	-0.2249381	3.84934133	6.05831179	2.73E-06	0.00013592	1.14568046
ENSMUSG00000072625	Gdf2	0.76929288	0.21044343	-0.5922389	-0.6488346	-0.2794082	NA	4.08597607	6.04171919	2.86E-06	0.00014101	0.76929288
ENSMUSG00000021047	Nova1	0.31776745	0.25105585	-1.1683632	-1.4820574	-0.1281685	-2.3731948	3.16140261	6.03910731	2.87E-06	0.00014103	-2.3731948
ENSMUSG00000078853	Igtp	-0.0921996	-0.6206572	NA	0.76744562	-0.2260441	NA	3.02337386	6.03647743	2.89E-06	0.00014123	0.76744562
ENSMUSG00000001240	Ramp2	0.1733493	-0.1510947	0.1105295	NA	0.71380192	1.07377802	3.17527082	5.8426658	4.82E-06	0.00022057	1.07377802
ENSMUSG00000027070	Lrp2	0.67926346	0.80169579	0.07944908	1.19399776	-0.2875944	3.13626045	4.0942076	5.78476055	5.60E-06	0.00025356	3.13626045
ENSMUSG00000041842	Fhdc1	-0.2389906	NA	-1.4833929	0.50406656	-0.1859801	0.71578367	3.94914748	5.74480251	6.22E-06	0.00027141	-1.4833929
ENSMUSG00000040631	Dok4	-0.2592744	-0.0555023	-0.2215207	-1.2671404	-0.2468921	2.26938777	7.56924821	5.73504263	6.38E-06	0.00027752	2.26938777
ENSMUSG00000032532	Cck	-0.7100512	-0.4184597	NA	-1.3081453	-0.9616844	NA	4.05800354	5.7298298	6.49E-06	0.00028143	-1.3081453
ENSMUSG00000031453	Rasa3	0.14905156	-1.780581	-0.3980858	1.51105847	0.58347023	1.60176324	4.64125685	5.68862322	7.20E-06	0.00030244	-1.780581
ENSMUSG00000048070	Pirt	-1.0451255	0.12402117	-0.2275995	-0.3542516	0.03483967	NA	3.89254205	5.67574512	7.48E-06	0.00031194	-1.0451255
ENSMUSG00000061288	Taok3	0.63063803	0.46083325	0.70866432	2.29344038	0.9739823	-1.4740271	4.03846335	5.65477485	7.87E-06	0.00032706	2.29344038
ENSMUSG00000019699	Akt3	0.1750148	0.80870492	0.00308971	1.16710018	1.35107787	1.12692526	3.77729401	5.60282434	9.02E-06	0.00037085	1.35107787
ENSMUSG00000097388	Gm3200	0.37028843	0.59813473	0.34533342	-0.4107264	1.04818225	0.91400236	3.90495141	5.50111183	1.18E-05	0.00046476	1.04818225
ENSMUSG00000050199	Lgr4	0.56143187	-0.1596794	0.5223471	2.28456927	0.76957118	0.02858346	4.55561431	5.48035594	1.24E-05	0.00048251	2.28456927
ENSMUSG00000034845	Plvap	-0.7454098	NA	0.77865034	0.87966981	0.10283319	1.60343288	3.17587121	5.44187114	1.37E-05	0.00052361	1.60343288
ENSMUSG00000026421	Csrp1	-0.0276883	-0.3165154	-0.6181312	0.36838506	0.22129755	1.15821283	8.06437014	5.42866111	1.42E-05	0.00054035	1.15821283
ENSMUSG00000018973	Hoxb1	-0.4551109	0.27055726	0.3686056	-0.87814	-0.1942958	-2.6036156	5.25576971	5.42241403	1.44E-05	0.0005474	-2.6036156
ENSMUSG00000064357	mt-Atp6	0.21184665	0.3884587	0.59423447	0.34596145	0.05354141	-0.1595123	6.68070156	5.38193771	1.60E-05	0.00059705	0.59423447
ENSMUSG00000079042	Apela	-0.4601203	0.78063596	0.2470427	1.73791746	-0.4971984	NA	3.12201627	5.36557651	1.67E-05	0.00061825	1.73791746
ENSMUSG00000006567	Atp7b	-0.1595433	-0.1761108	-1.2195938	1.64178189	0.18629416	NA	4.36565612	5.33724147	1.80E-05	0.00065856	1.64178189
ENSMUSG00000031529	Tnks	0.25240478	0.08426327	0.54159305	0.6971778	0.46712902	0.23003053	5.97444127	5.33607713	1.81E-05	0.00065857	0.6971778
ENSMUSG00000044337	Ackr3	-0.4881413	0.16162805	0.94288691	-0.7521332	1.1122966	0.99871223	4.19093524	5.31736647	1.90E-05	0.00068523	1.1122966
ENSMUSG00000074743	Thbd	-0.1674615	0.40545902	NA	-0.1283794	1.36636307	1.0460049	3.18138014	5.28422755	2.07E-05	0.00074025	1.36636307
ENSMUSG00000006675	P4htm	-0.0349355	-0.0268448	-0.1492971	-0.9380593	0.72652761	NA	3.9169846	5.27527124	2.12E-05	0.00075469	-0.9380593
ENSMUSG00000015143	Actn1	-0.1307007	-0.411464	-0.7798476	0.77214699	-0.2558027	-0.2368662	5.31970202	5.22668382	2.40E-05	0.00084955	-0.7798476
ENSMUSG00000022367	Has2	-0.1831583	1.00420056	0.46017054	0.12441024	0.94919907	-0.7347791	5.33391828	5.17100431	2.78E-05	0.0009537	1.00420056
ENSMUSG00000097910	5033428I22R	0.63223363	0.0226458	0.0945401	1.93672153	0.89033765	NA	3.66759283	5.11815465	3.18E-05	0.00106348	1.93672153
ENSMUSG00000001504	Irx2	-0.7041791	0.961558	-0.8328434	-1.86714	-0.3961645	0.11555148	4.63327111	4.92699007	5.22E-05	0.00164745	-1.86714
ENSMUSG00000030122	Ptms	-0.3917163	-0.3883396	-0.413718	0.26451976	-0.005925	-0.6194166	5.39103253	4.92432326	5.25E-05	0.0016545	-0.6194166
ENSMUSG00000057751	Megf6	0.53206569	NA	-0.2282247	NA	-0.1100173	0.73059889	2.99192794	4.92164577	5.29E-05	0.00165793	0.73059889
ENSMUSG00000036602	Alx1	1.12935848	0.10235565	0.41904845	0.92918527	-0.3058923	-0.813932	4.42687105	4.90102623	5.58E-05	0.00171668	1.12935848
ENSMUSG00000098761	Gm18821	0.18113295	0.58761708	-0.1199029	NA	0.27666397	0.69770726	5.35893016	4.88347703	5.84E-05	0.00177328	0.69770726
ENSMUSG00000027447	Cst3	0.11449882	0.1775218	-0.0501558	0.70197714	0.53915676	0.03156579	8.47878564	4.80959691	7.06E-05	0.00208538	0.70197714
ENSMUSG00000019158	Tmem160	-0.1874383	0.15296294	-0.5501217	1.39452426	-0.2585483	-0.3059455	5.35990449	4.80899849	7.07E-05	0.00208538	1.39452426

ID	Gene	v1	v2	v3	v4	v5	v6	v7	v8	v9	v10	v11
ENSMUSG00000038530	Rgs4	0.43148625	0.49528899	0.3323453	1.18732114	0.75843346	NA	5.10173256	4.76815042	7.85E-05	0.00227187	1.18732114
ENSMUSG00000030374	Strn4	-0.3591765	-0.4371724	-0.6659261	-0.1411365	-0.2273589	-0.1396915	6.30075023	4.75845805	8.05E-05	0.00232358	-0.6659261
ENSMUSG00000024868	Dkk1	0.26444933	0.46028318	1.46530968	NA	0.45231554	-0.5220517	4.90578209	4.75022541	8.22E-05	0.00234707	1.46530968
ENSMUSG00000031636	Pdlim3	0.28027536	0.56210418	0.28359038	0.13225456	1.14403761	NA	5.48223289	4.72501483	8.77E-05	0.00247615	1.14403761
ENSMUSG00000026305	Lrrfip1	0.16362009	0.11953924	0.11269009	0.07676434	0.53763508	0.88313643	6.76150948	4.72435589	8.79E-05	0.00247615	0.88313643
ENSMUSG00000027495	Fam210b	0.10509222	0.43434765	0.20600933	1.16986346	1.24515447	0.69067847	4.59817194	4.72358598	8.81E-05	0.00247615	1.24515447
ENSMUSG00000019851	Perp	0.31267455	0.00527226	0.01029095	1.80865563	0.9475345	NA	4.45599292	4.71482651	9.01E-05	0.0025207	1.80865563
ENSMUSG00000022836	Mylk	0.64095258	-0.0216275	0.63100169	2.23140851	-0.1461599	NA	3.25855512	4.69088823	9.58E-05	0.0026618	2.23140851
ENSMUSG00000002944	Cd36	0.34343292	0.79608648	0.32647588	0.4725733	-0.1497983	-2.8542025	3.641473	4.65236185	0.00010571	0.00291118	-2.8542025
ENSMUSG00000024515	Smad4	-0.6065681	-0.8098421	-0.1600377	-0.2135099	-0.2163289	-0.3752059	5.59245439	4.65048507	0.00010622	0.00291545	-0.8098421
ENSMUSG00000027254	Map1a	-0.2341333	0.79334154	-0.5493813	0.66344819	1.022578	1.46294714	4.45220304	4.61939172	0.00011502	0.00313186	1.46294714
ENSMUSG00000038319	Kcnh2	0.02920913	0.10754932	-0.103345	-0.71873	-0.0810356	-2.7864161	5.30542898	4.60855988	0.00011825	0.00319825	-2.7864161
ENSMUSG00000083563	Gm13340	0.22005415	0.15857796	0.34835212	0.48544446	0.2363407	0.61513094	4.88958914	4.59293014	0.00012307	0.00332123	0.61513094
ENSMUSG00000104083	Gm29739	0.21886914	1.23415606	0.22831733	0.35470935	0.29669797	-0.0188308	3.81971693	4.56528941	0.00013208	0.00349895	1.23415606
ENSMUSG00000028024	Enpep	-0.0229177	-1.0952285	0.31479349	-2.2150995	-0.2356646	NA	3.39420101	4.56529897	0.00013226	0.00349895	-2.2150995
ENSMUSG00000044147	Arf6	-0.2800212	-0.1947359	-1.1125265	-0.7807477	-0.1054201	-0.3685243	4.46731128	4.51552111	0.00014997	0.00389087	-1.1125265
ENSMUSG00000021765	Fst	-0.0733429	0.62546885	0.7395554	NA	0.82856474	0.40630197	4.91402662	4.49512579	0.00015798	0.00403795	0.82856474
ENSMUSG00000028949	Smarcd3	-0.1488085	-0.2568183	-0.6815835	1.3040751	-0.2622562	-1.2824139	5.52986807	4.47544683	0.0001661	0.00421889	1.3040751
ENSMUSG00000086324	Gm15564	0.0386071	0.84464244	0.87318332	0.34698556	0.20340748	0.8482499	3.7760791	4.44146186	0.00018142	0.00450857	0.87318332
ENSMUSG00000043008	Klhl6	-0.296785	-0.3179399	1.27459861	-1.7550947	0.80857837	0.42077406	4.36233436	4.43250646	0.0001853	0.00456258	-1.7550947
ENSMUSG00000001995	Sipa1l2	-0.2037007	-0.0660577	-0.248338	-0.8048231	0.99119586	NA	4.91342755	4.4269323	0.00018794	0.00460898	0.99119586
ENSMUSG00000040289	Hey1	0.10928164	1.2799991	0.60279406	0.87341921	0.8021102	1.0706577	4.52086358	4.42443718	0.00018914	0.00461959	1.2799991
ENSMUSG00000038473	Nos1ap	0.65201146	-0.6421831	0.40492721	0.08907096	0.75089699	-0.7674045	4.06823081	4.39499658	0.00020384	0.00488342	-0.7674045
ENSMUSG00000030110	Ret	-0.5595629	NA	-0.3863967	-2.6615312	-0.3836555	NA	3.5548283	4.38042175	0.00021153	0.00504429	-2.6615312
ENSMUSG00000028245	Nsmaf	-0.4095902	-0.5716481	-0.2053678	-0.7040496	-0.1677065	0.22076548	6.11340346	4.36577943	0.00021955	0.00521487	-0.7040496
ENSMUSG00000029765	Plxna4	-0.334198	-0.3318999	-0.2921521	1.00302672	0.48962312	NA	4.39254277	4.35957377	0.00022332	0.00529397	1.00302672
ENSMUSG00000018427	Ypel2	0.12767868	0.25698743	-0.4491109	1.6956045	-0.1475659	2.58006502	4.64505589	4.35512314	0.00022557	0.00531612	2.58006502
ENSMUSG00000084274	Gm12504	0.49379363	0.72726889	0.6080864	1.63493681	0.25504479	0.68376509	3.33858668	4.33730389	0.00023601	0.00551902	1.63493681
ENSMUSG00000034101	Ctnnd1	0.08433459	0.08770795	0.30295703	0.87547607	0.86764655	-0.1502512	3.69332744	4.33296023	0.00023862	0.00556941	0.87547607
ENSMUSG00000055044	Pdlim1	0.17287955	-0.1097257	0.28158076	0.58879995	0.72359423	0.91487542	5.93877294	4.32472052	0.00024366	0.00567608	0.91487542
ENSMUSG00000020024	Tns3	0.81948571	-0.0159482	0.16123033	-2.0791109	0.1392211	0.96413344	3.42546021	4.32218636	0.00024523	0.00569319	-2.0791109
ENSMUSG00000020032	Nuak1	0.806954	-0.1356974	-0.5011112	1.16270312	0.7728432	1.01186555	3.35326246	4.32201714	0.00024534	0.00569319	1.16270312
ENSMUSG00000105655	Gm42659	0.25770322	0.5558484	-0.7949808	1.33247611	-0.3992035	1.82041628	3.23295364	4.31310376	0.00025095	0.00580106	1.82041628
ENSMUSG00000082575	Gm13050	0.18519918	0.78900256	0.20092829	0.15934546	0.14625234	-0.2031075	5.99966082	4.30982205	0.00025304	0.00583836	0.78900256
ENSMUSG00000029550	Sppl3	-0.3843974	-0.6107381	-0.3947105	0.11438596	-0.5077308	0.39157068	4.99833834	4.29656536	0.00026169	0.00600348	-0.6107381
ENSMUSG00000078185	Chml	0.20764935	-0.5341374	0.65705251	-0.3229717	-0.2977883	2.7864399	3.79680272	4.29516624	0.00026262	0.00601339	2.7864399
ENSMUSG00000032035	Ets1	-0.3762576	-1.5298776	-0.4050718	NA	0.07978456	-0.7164611	3.37360805	4.28719744	0.00026815	0.00610526	-1.5298776
ENSMUSG00000025255	Zfhx4	-0.0229743	-0.6744564	-0.2523985	NA	-0.0860714	-0.9108566	3.35932148	4.28530641	0.00026943	0.00612304	-0.9108566
ENSMUSG00000039611	Tmem246	0.60183355	0.3806814	-0.1543308	1.76613651	0.57055039	-0.845336	5.66311777	4.27145381	0.00027888	0.00626811	1.76613651
ENSMUSG00000027559	Car3	0.15184785	1.07500656	0.9290689	1.72075023	-0.1733896	-1.1297804	4.84195592	4.27137976	0.00027893	0.00626811	1.72075023
ENSMUSG00000060187	Lrrc10	0.33001442	0.88750793	0.26536173	-0.8725191	0.78207614	NA	6.0164626	4.26364393	0.00028478	0.00636423	0.88750793
ENSMUSG00000032841	Prr5l	-0.0859989	-1.0568758	-0.3281402	NA	1.02364013	-0.6258812	3.99658037	4.25980149	0.00028722	0.0064069	-1.0568758
ENSMUSG00000037553	Zdhhc18	-0.696244	-0.1776953	-0.5385595	-1.9438628	-0.3787355	-1.6073385	3.80876831	4.2255628	0.00031321	0.00691002	-1.9438628
ENSMUSG00000050777	Tmem37	-0.8068419	0.44612094	-0.9106175	-1.0401614	0.39035243	0.9771424	3.54607072	4.22029464	0.00031741	0.0069764	-1.0401614
ENSMUSG00000032291	Crabp1	0.27445126	0.30967236	0.45767204	0.00060881	-0.1044123	-1.3977955	8.13887927	4.19311299	0.00034011	0.00734273	-1.3977955
ENSMUSG00000054555	Adam12	0.61236495	0.73598891	-0.0018426	0.4365259	1.09851047	NA	3.66239569	4.19131672	0.00034265	0.00737115	1.09851047
ENSMUSG00000070407	Hs3st3b1	-0.8242637	-0.4819567	-0.1566569	1.95697386	0.23487794	-0.0062357	4.26714077	4.18400796	0.00034788	0.00745713	1.95697386
ENSMUSG00000021262	Evl	0.0567526	-0.9939405	-0.4542538	0.71939604	-0.5527506	-0.8659822	3.40514425	4.11713994	0.00041177	0.00850984	-0.9939405
ENSMUSG00000067925	Cxx1a	-0.0193237	-0.2957956	-0.6376181	1.56604083	0.23751616	0.25549933	4.10958194	4.11554283	0.00041343	0.00852956	1.56604083
ENSMUSG00000006576	Slc4a3	-0.4517589	0.38474332	0.93000783	-1.4684342	0.24250023	2.07825344	3.63394755	4.11408183	0.00041495	0.00854642	2.07825344
ENSMUSG00000009681	Bcr	0.11217275	0.04418385	-1.309868	-0.1607143	0.4696503	0.24796288	5.63114416	4.104261	0.00042534	0.00873063	-1.309868
ENSMUSG00000034205	Loxl2	0.1350319	0.9792886	-0.1969657	-0.1101991	0.16041144	1.33034839	4.60565831	4.07766311	0.00045478	0.00914855	1.33034839
ENSMUSG00000022708	Zbtb20	0.35230273	0.02178002	0.23596002	2.35843365	0.50726959	0.51593393	5.79972735	4.02443246	0.00051986	0.010253	2.35843365
ENSMUSG00000036292	Gramd1c	-0.3895421	-0.6606721	0.38518012	-0.9681197	-0.4224283	NA	4.91899108	3.98258335	0.00057739	0.0113542	-0.9681197
ENSMUSG00000026888	Grb14	-0.0696995	-0.1038993	-0.2252089	-0.7532958	0.27041414	NA	5.27271116	3.96248864	0.0006072	0.01159725	-0.7532958
ENSMUSG00000043439	E130012A19Rik	-0.5534942	-0.9602478	-0.6462931	0.49190465	-0.329313	-0.4944212	3.96697039	3.94951001	0.00062725	0.01194254	-0.9602478
ENSMUSG00000004885	Crabp2	0.11342986	-0.2515866	0.47980102	0.35416109	-0.5558132	-1.990537	4.86139771	3.94096546	0.00064081	0.01217606	-1.990537
ENSMUSG00000036862	Dchs1	1.04389629	0.40788878	-0.1817068	0.62791786	0.00149264	0.44349137	3.98915773	3.92499555	0.00066693	0.01255943	1.04389629
ENSMUSG00000061082	Plac1	-0.2908223	-0.6028602	-0.4270481	0.18239694	-0.156774	NA	4.07984496	3.90825028	0.00069612	0.01293983	-0.6028602
ENSMUSG00000059741	Myl3	-0.0816753	1.19492349	0.38310084	0.40340811	0.59623423	NA	9.60198973	3.90765004	0.00069676	0.01293983	1.19492349
ENSMUSG00000059430	Actg2	0.39758065	0.59167851	-0.8366069	-0.4790023	-0.3516616	NA	5.14917037	3.88988403	0.00072879	0.01345199	-0.8366069
ENSMUSG00000060860	Ube2s	-0.0627931	-0.4428138	-0.5451237	-0.2981935	-0.0003601	-0.7741743	5.43072984	3.87581197	0.00075442	0.01383501	-0.7741743
ENSMUSG00000018819	Lsp1	0.15061957	0.15680146	0.30482916	-0.8253506	0.32464444	-2.2179152	5.25850566	3.87375088	0.00075801	0.01386428	-2.2179152
ENSMUSG00000045039	Megf8	0.41763693	-0.5095315	0.10434934	-2.3175407	0.42327396	-1.3666256	3.82458947	3.86029452	0.00078388	0.01414501	-2.3175407
ENSMUSG00000052854	Nrk	-0.1842742	-0.1266387	1.05194034	-1.1497934	0.08903049	NA	3.75147828	3.85630183	0.00079173	0.01426527	-1.1497934
ENSMUSG00000015759	Nkx2-5	-0.0165285	0.24010382	0.92998072	-0.2259559	0.08599546	-0.210323	7.85153206	3.83521911	0.00083459	0.01477333	0.92998072
ENSMUSG00000096780	Tmem181b-ps	-0.0628764	0.76261616	0.84224928	1.24233827	0.14749136	-0.4485101	4.0589472	3.83232495	0.00084049	0.01482955	1.24233827
ENSMUSG00000080316	Spaca6	0.96236533	-0.1500988	0.34387173	1.08596762	0.90848692	NA	3.62705599	3.82626785	0.00085326	0.01495064	1.08596762
ENSMUSG00000058301	Upf1	-0.2785619	-0.5439148	-0.6309245	0.21913047	-0.6517643	-0.0950272	4.24761712	3.80823706	0.00089244	0.01543573	-0.6517643
ENSMUSG00000081302	Gm12020	0.18744815	-0.0572826	0.15777792	NA	0.00539801	1.13614155	5.81370553	3.80534406	0.00089932	0.01553254	1.13614155
ENSMUSG00000035239	Neu3	0.00363253	-0.9780234	0.38609215	0.33433667	-0.1110601	NA	3.35687771	3.8038432	0.00090225	0.01556091	-0.9780234
ENSMUSG00000024805	Pcgf5	-0.0331679	-0.1181054	-0.0813827	-0.1613648	0.73526058	2.0007595	5.73662121	3.80306889	0.00090399	0.01556871	2.0007595
ENSMUSG00000028011	Tdo2	-0.0242624	-1.7244582	-0.5853216	0.83222197	-0.4088917	NA	4.22677496	3.78745692	0.00094064	0.0160399	-1.7244582
ENSMUSG00000021200	Asb2	-0.020309	-0.0571794	0.72217414	-0.9188996	0.89591271	NA	7.37574989	3.78481671	0.00094612	0.01608797	-0.9188996
ENSMUSG00000028289	Epha7	0.04540586	0.00357668	0.86888122	-0.1011506	0.03572906	-1.4012834	6.1095564	3.77871472	0.00096043	0.01626279	-1.4012834
ENSMUSG00000023904	Hcfc1r1	-0.0575572	0.95806039	-0.4431174	-0.5311414	0.07410348	0.27858687	6.02597865	3.7741462	0.0009714	0.01642549	0.95806039
ENSMUSG00000045776	Lrtm1	-0.2695706	0.78605986	NA	-0.9841152	0.8366783	NA	3.40401756	3.76936515	0.00098301	0.01657543	-0.9841152
ENSMUSG00000029426	Scarb2	0.35135894	-0.4037501	-0.7252452	2.51854874	-0.3436762	1.68166334	3.80294756	3.7663197	0.00099047	0.01667805	2.51854874
ENSMUSG00000021702	Thbs4	-0.0042218	0.11694548	-0.4623848	2.39482167	0.97055891	NA	8.36464772	3.75134462	0.00102836	0.01712519	2.39482167
ENSMUSG00000006221	Hspb7	0.02701911	0.69726762	-0.1526366	0.69253385	1.01610855	NA	6.87229891	3.74151081	0.00105341	0.01742241	1.01610855
ENSMUSG00000025776	Crispld1	-0.5774506	-0.0908151	0.28805327	NA	-0.3960987	-0.6641027	4.12647098	3.73526073	0.00107036	0.01767854	-0.6641027
ENSMUSG00000025932	Eya1	-0.7025263	NA	-0.2489991	NA	0.51887641	1.05992047	3.81244626	3.73022722	0.00108331	0.01781938	1.05992047
ENSMUSG00000014329	Bicc1	0.99556663	0.09774859	-0.2099706	-0.4315827	-0.199294	0.97771974	3.02622418	3.71447054	0.00112647	0.01835454	0.99556663
ENSMUSG00000036833	Pnpla7	-0.5014837	-0.2708724	1.08759388	NA	0.41521978	-0.7472915	3.22609645	3.70738674	0.00114642	0.01860439	1.08759388
ENSMUSG00000059456	Ptk2b	0.13723968	0.62959069	0.81257821	0.42477934	0.76207061	NA	5.14125163	3.69228092	0.00119013	0.01917274	0.81257821
ENSMUSG00000022353	Mtss1	0.62663456	0.16527495	0.19186232	0.95165596	0.48259073	0.0531688	4.63520233	3.68980509	0.00119745	0.01925159	0.95165596
ENSMUSG00000011427	Zfp790	-0.2220908	0.62345158	0.52266709	1.08433672	-0.0062801	2.87912141	3.75560978	3.66926859	0.00125988	0.02009498	2.87912141
ENSMUSG00000060336	Zfp937	0.5382898	-0.2856524	1.00689697	0.54063766	-0.4584721	1.00942914	3.81230083	3.65012222	0.00132096	0.0209912	1.00942914
ENSMUSG00000045193	Cirbp	0.37015788	0.41989175	-0.2583417	0.86721277	0.20105451	-0.5950168	5.20812541	3.63285317	0.00137854	0.02181404	0.86721277
ENSMUSG00000060913	Trim55	0.22795805	0.642657	-0.4862149	0.73594319	0.57812363	NA	6.04284169	3.62447214	0.00140851	0.02218225	0.73594319
ENSMUSG00000074227	Spint2	-0.8740298	-0.3033028	0.46160353	-0.4397556	0.1073919	0.60271664	4.03532642	3.62397302	0.0014091	0.02218225	-0.8740298
ENSMUSG00000050315	Synpo2	-0.1762586	0.54611509	0.75003488	-0.888158	0.12016245	2.05523067	5.00896214	3.61134135	0.00145371	0.02273658	2.05523067
ENSMUSG00000040659	Efhd2	-0.1333907	-0.4554024	-0.4308446	1.19179043	0.12328167	1.02952776	6.2285853	3.60131463	0.00149011	0.0231859	1.19179043
ENSMUSG00000036639	Nudt1	-0.1840091	0.36809663	-0.599636	0.19295452	0.00093433	1.46264072	4.88724805	3.59055002	0.00153018	0.02368748	1.46264072

24

ID	Gene											
ENSMUSG00000079659	Tmem243	0.36913722	0.48239204	-0.0065465	1.65646762	-0.0928693	1.11056805	5.00595964	3.58578907	0.00154824	0.02387532	1.65646762
ENSMUSG00000045877	4933415A04F	-0.2841008	-0.846953	-0.4500602	1.33840651	-0.5831616	-0.2552296	3.84511426	3.57070312	0.00160686	0.02455197	1.33840651
ENSMUSG00000030491	Tdrd12	0.84250167	-0.0863407	0.63350757	0.69183618	-0.2350402	NA	3.68991634	3.57049817	0.00160767	0.02455197	0.84250167
ENSMUSG00000026748	Plxdc2	-0.6939045	0.65195159	0.88541335	-1.311909	-0.0850775	0.18887767	3.63220763	3.55835717	0.00165644	0.02500167	-1.311909
ENSMUSG00000057691	Zfp746	0.09280795	-0.167723	-0.6289098	2.13221343	0.05268187	2.59492525	3.93300909	3.54761747	0.00170079	0.02557526	2.59492525
ENSMUSG00000033066	Gas7	-0.5209383	0.9008574	-0.2746878	-0.0033251	0.91240186	0.90388019	3.97107422	3.47241842	0.00204562	0.02958316	0.91240186
ENSMUSG00000039195	1110008P14F	-0.2057477	0.91963519	-0.253783	-0.0016909	0.09155044	1.26865497	4.5058489	3.45454786	0.00213714	0.0307544	1.26865497
ENSMUSG00000027820	Mme	0.74912607	0.13830038	0.23558184	0.37400678	0.1733173	-0.2029413	5.85837433	3.4449276	0.00218806	0.03108531	0.74912607
ENSMUSG00000034295	Fhod3	-0.0466497	0.58959908	0.67133406	-1.7748687	-0.1697193	0.77400545	4.85673086	3.44120743	0.00220806	0.03133271	-1.7748687
ENSMUSG00000042594	Sh2b3	-0.1445	0.18068352	-0.4443063	0.0719263	-0.10794	2.58856308	4.8076199	3.43835956	0.0022235	0.03144104	2.58856308
ENSMUSG00000000811	Txnrd3	-0.6027264	-1.2247236	-0.0298026	-0.2535138	0.67170672	0.62671632	3.41163725	3.43422058	0.00224612	0.03168681	-1.2247236
ENSMUSG00000024883	Rin1	-0.6578541	-0.5453574	0.21710648	-1.220337	0.14050333	1.85753939	3.53852304	3.43036697	0.00226739	0.03189173	1.85753939
ENSMUSG00000083192	Rpl31-ps12	0.35329009	0.54393607	0.28499351	0.41133895	0.32652752	0.68412142	3.43802196	3.42976885	0.0022707	0.03189173	0.68412142
ENSMUSG00000076258	Gm23935	-0.1220826	0.3120257	0.11184905	0.25331883	0.0734733	-1.4418269	5.38991253	3.41105343	0.00237697	0.03314139	-1.4418269
ENSMUSG00000020160	Meis1	0.22336453	0.03846038	0.08848156	-0.1053248	0.10506354	-1.201856	7.15809267	3.40985324	0.00238394	0.03314139	-1.201856
ENSMUSG00000034908	Sidt2	-0.2090886	-0.6660573	-0.9204258	-0.3443647	-0.4450191	0.12061653	4.7555857	3.39832811	0.00245198	0.03383117	-0.9204258
ENSMUSG00000069376	Gm5507	0.05766129	0.79807095	-0.0733969	0.09277944	0.23432759	0.09290173	4.05780498	3.37736821	0.00258061	0.03529367	0.79807095
ENSMUSG00000020211	Sf3a2	-0.0646137	-0.3307047	-0.3353707	0.82428658	-0.0680151	0.09430095	6.166215	3.37638154	0.00258683	0.0353387	0.82428658
ENSMUSG00000022790	Igsf11	-0.1856417	-0.4561375	-0.143417	1.88427933	0.08618287	2.37898665	3.9648263	3.36102835	0.00268545	0.036562	2.37898665
ENSMUSG00000041895	Wipi1	0.02658079	1.06834637	0.57146847	0.08044334	0.84093559	0.03253186	4.34806089	3.35897287	0.00269893	0.03670418	1.06834637
ENSMUSG00000028426	Rad23b	-0.1092735	-0.478501	-0.1167132	0.58838319	-0.1339332	0.00176516	6.41231625	3.35542583	0.00272234	0.03698103	0.58838319
ENSMUSG00000040520	Manea	0.49048582	-0.1483532	0.78421673	-0.200359	0.10427709	0.71410292	4.78168662	3.3472873	0.00277682	0.03763651	0.78421673
ENSMUSG00000003411	Rab3b	0.02198479	-0.1239647	-0.1459263	0.61370915	1.13023329	-1.0867101	4.57650208	3.34112484	0.00281878	0.03811975	1.13023329
ENSMUSG00000043618	Eif5a3-ps	-0.1550257	0.19724866	0.59295995	0.02580133	0.41274082	-0.1561297	7.9468675	3.33650488	0.00285089	0.03842497	0.59295995
ENSMUSG00000042978	Sbk1	-0.7117235	0.88103319	0.49697839	0.61000455	-0.109848	0.54847062	4.32146088	3.33237172	0.00287945	0.03870792	0.88103319
ENSMUSG00000026678	Rgs5	0.21640152	-0.3025492	0.4421354	0.46097424	0.64021769	0.40893114	6.80214508	3.33199713	0.00288244	0.03870792	0.64021769
ENSMUSG00000010529	Gm266	0.38375715	NA	0.19199172	-1.3404643	0.25130396	0.98185178	3.5950752	3.33122958	0.00288746	0.03870792	-1.3404643
ENSMUSG00000053897	Slc39a8	0.53699213	-0.3819096	0.00474337	0.74440111	0.09542412	0.85114537	5.61613451	3.33116823	0.00288789	0.03870792	0.85114537
ENSMUSG00000033721	Vav3	-0.4489964	0.43377913	0.03410925	0.8421381	0.25747334	NA	3.57847926	3.33027775	0.00289415	0.03872241	0.8421381
ENSMUSG00000025491	Ifitm1	0.0179804	0.76278099	0.58924878	0.4753955	0.12543163	0.39289405	7.72172948	3.33019244	0.00289537	0.03872241	0.76278099
ENSMUSG00000042613	Pbxip1	0.05389461	0.63172007	-0.3298975	0.46433862	0.88601709	0.60132985	5.28276974	3.32378803	0.00294017	0.03919153	0.88601709
ENSMUSG00000029108	Pcdh7	0.1335165	-0.0317946	0.24258208	0.17054259	0.62005085	1.23777637	5.63239141	3.32295443	0.00294614	0.03922777	1.23777637
ENSMUSG00000060935	Tmem263	-0.0312005	-0.0261015	0.08723821	0.21920149	0.7095984	0.24102919	6.0887167	3.32174528	0.00295481	0.03929996	0.7095984
ENSMUSG00000021068	Nin	0.89727339	-0.259986	0.17744229	1.02330162	-0.479192	-0.0411713	3.4453805	3.32091511	0.00296078	0.03933606	1.02330162
ENSMUSG00000000078	Klf6	-0.1352732	-0.0767433	0.12045505	-0.0943603	0.66548769	0.13106502	6.51126157	3.30068895	0.00310988	0.04077925	0.66548769
ENSMUSG00000029864	Gstk1	-0.5450687	0.26903017	0.81577494	0.92524963	0.20054342	-1.2864481	3.21876403	3.28740586	0.00321176	0.04188806	-1.2864481
ENSMUSG00000030245	Golt1b	0.27313661	-0.0312344	0.00709977	0.59331899	-0.0005561	0.26747472	7.59134502	3.280661	0.00326474	0.04239602	0.59331899
ENSMUSG00000078350	Smim1	-0.0416044	-0.3795568	0.15822456	-0.7694006	0.17635939	NA	4.78843564	3.26266492	0.00341029	0.04400257	-0.7694006
ENSMUSG00000005575	Ube2m	-0.0924425	-0.3052918	-0.6078645	0.28975244	0.09960172	0.04280276	5.93968515	3.25422031	0.00348075	0.04472085	-0.6078645
ENSMUSG00000034687	Fras1	0.18911708	0.16193089	0.33129671	3.32832727	0.45264311	-0.6279164	4.66330243	3.24274824	0.00357876	0.04573702	3.32832727
ENSMUSG00000026792	Lrsam1	0.00862128	0.03600525	-0.0053302	0.79368694	0.77290164	2.58840065	3.40971635	3.21027111	0.00387104	0.04905756	2.58840065
ENSMUSG00000015968	Cacna1d	0.4534959	0.23051045	0.0608757	1.36366053	0.36847035	1.43786747	5.70208565	3.20675494	0.00390405	0.04920707	1.43786747